

Calcareous nannofossils from the Paleogene equatorial Pacific (IODP Expedition 320 Sites U1331-1334)

Paul R. Bown

Department of Earth Sciences, University College London, Gower Street, London, WC1E 6BT, UK; p.bown@ucl.ac.uk

Tom Dunkley Jones

School of Geography, Earth and Environmental Sciences, University of Birmingham, Edgbaston, Birmingham, B15 2TT, UK

Manuscript Received 11th November, 2011; Manuscript Accepted 12th April, 2012.

Abstract Integrated Ocean Drilling Program Expedition 320 cored six sites and 16 holes (Sites U1331-U1336) as part of the Pacific equatorial age transect, recovering a virtually complete composite section ranging from upper Pleistocene to lower Eocene. In general, the successions comprise abyssal biogenic sediments with nannofossil- and radiolarian-ooze end members. Stratigraphic highlights include recovery of richly nannofossiliferous Oligocene successions and complete Eocene/Oligocene and Oligocene/Miocene boundaries at four sites: U1331 through U1334 and U1332 through U1336, respectively. Here, we present a taxonomic overview of the Paleogene nannofossil assemblages from Sites U1331-1334, illustrating 163 taxa and including the description of 11 new species (*Reticulofenestra moorei*, *Reticulofenestra westerholdii*, *Coccolithus scheri*, *Cruciplacolithus? klausii*, *Calcidiscus? edgariae*, *Calcidiscus? kamikurii*, *Helicosphaera robinsoniae*, *Pedinocyclus gibbsiae*, *Discoaster williamsii*, *Sphenolithus kempii*, *Sphenolithus richteri*, *Sphenolithus peartiae*) and two new combinations (*Calcidiscus? detectus*, *Coccolithus biparteoperculatus*).

Keywords Paleogene, Eocene, Oligocene, Pacific, taxonomy, calcareous nannofossils

1. Introduction

Integrated Ocean Drilling Program Expedition (IODP Exp.) 320 (March-May 2009) cored six sites and 16 holes (Sites U1331-U1336; Figure 1) as part of the Pacific equatorial age transect (PEAT), recovering a virtually complete composite section ranging from upper Pleistocene to lower Eocene, representing 51 Ma of Earth history. The main objective of the PEAT is to study key intervals of Cenozoic climate history via a transect of sites all drilled at the palaeo-Equator. The drilling strategy was optimised to enhance the recovery of the calcareous sediments required for many palaeoceanographic proxy methodologies. This was achieved by targeting sediments that were deposited above the carbonate compensation depth (CCD) on what was young, shallow crust near to the East Pacific Rise ridge axis. These sediment packages were subsequently transported away from the ridge axis by the north-westward drift of the Pacific plate (Pälike *et al.* 2010), such that sites targeting the oldest intervals (early/middle Eocene), were furthest from the modern ridge axis and situated on the oldest/deepest oceanic crust and those targeting more recent intervals (Miocene) were closer to the modern ridge axes on young/shallow crust.

The youngest 12 million year portion of the Exp. 320 record (middle Miocene to Recent) was only well represented at Site U1335 and elsewhere only present as a relatively thin (5-12m) veneer of non-calcareous brown clay (Figure 2). The targeted lower Eocene to lower Miocene stratigraphy, however, was well recovered and comprises a continuous succession of biogenic sediments, with nannofossil- and radiolarian-ooze end members, across this interval. Chert and porcellanite levels were present in the lower parts of Sites U1331, U1332 and U1336, whilst turbidites (with reworked microfossils) were present in limited horizons at Sites U1331 and U1335. All the sites contribute near-continuous successions to the overall composite section, with stratigraphic highlights

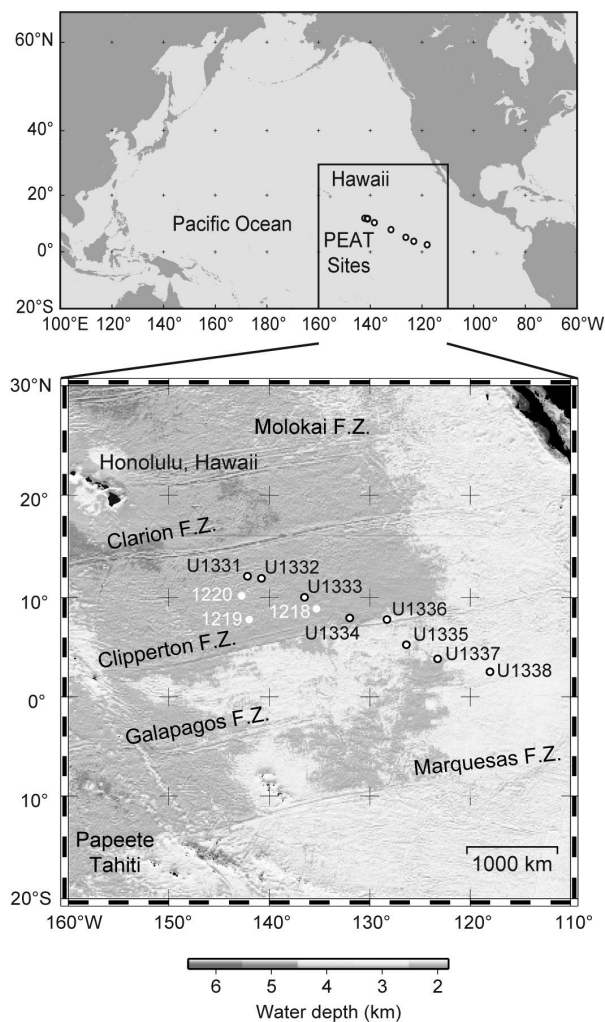


Figure 1. Location map of the sites drilled during IODP Expeditions 320 and 321. Previous DSDP and ODP sites are shown in white. F.Z. = fracture zone. The positions of Honolulu and Papeete are indicated for orientation (after Pälike *et al.*, 2010).

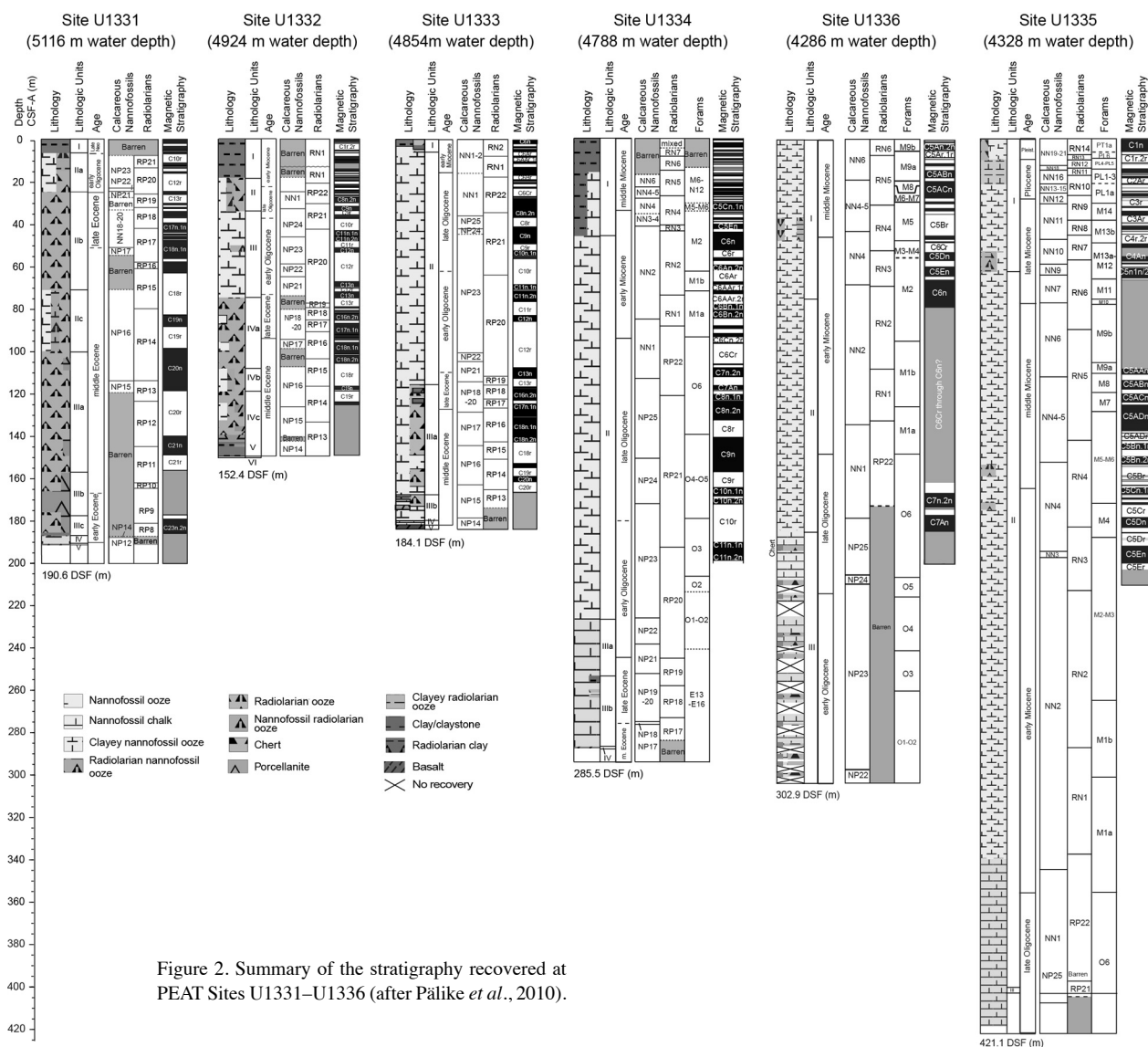


Figure 2. Summary of the stratigraphy recovered at PEAT Sites U1331–U1336 (after Pálike *et al.*, 2010).

including the recovery of complete Eocene/Oligocene and Oligocene/Miocene boundaries at four sites: U1331 through U1334 and U1332 through U1336, respectively. The complementary IODP Expedition 321 (May–July 2009) cored a further two sites (Sites U1337–1338), as an integral part of the PEAT, focussing on the Miocene–Pleistocene interval. This completed the recovery of a continuous section of early Eocene to Pleistocene sediments from beneath the Pacific palaeo-equator (Pálike *et al.* 2010). These sections provide excellent records of the biotic response to periods of rapid environmental change in the principal phytoplanktonic and zooplankton groups and the benthic foraminifera.

Initial biostratigraphic results are published in Pálike *et al.* (2010) and high resolution integrated stratigraphic, isotopic and palaeoecological studies are in progress. In this paper, we present a taxonomic overview of the Palaeogene nannofossil assemblages from Sites U1331–1334, illustrating 163 taxa and including the description of 11 new species and three new combinations.

2. Material and methods

Nannofossils were viewed in simple smear-slides (Bown and Young, 1998), using transmitted-light microscopy (Zeiss Axiophot) in cross-polarised (XPL) and phase-contrast (PC) light at x1000–1600.

3. Biostratigraphy

Semi-quantitative biostratigraphic data was generated during Exp. 320 drilling and the stratigraphic range charts for sites U1331–1334, presented here as Charts 1 through 4, incorporate these data with some post-expedition revisions. In the Paleogene part of the section the nannofossil biozonation of Martini (1971) was used and all standard nannofossil biozones were recognised (Zones NP12–NP25). At these equatorial sites, however, the temperate-high latitude favouring taxa *Isthmolithus recurvus* and *Chiasmolithus oamaruensis* were rare and sporadically distributed, and so the upper Eocene zones NP18–20 could not be reliably distinguished (Pálike *et al.*, 2010). Further discussion of biostratigraphically significant taxa is included in Pálike *et al.* (2010) and the Systemic Palaeontology section that follows herein.

4. Preservation and the CCD

The dominant Paleogene lithologies recovered during Exp. 320 were biogenic oozes but the nature of the preserved sedimentary record varies dramatically through the succession. The dominant controls on this variation appears to be the extent of water-column and seafloor dissolution, principally of calcareous microfossils, related to the changing carbonate saturation state of Pacific deepwaters, together with changes in the nature and export rates of original biotic production. The strength of the carbonate dissolution signal is a direct result of the palaeodepth histories of these abyssal sites, with sedimentation commencing above the CCD on newly formed oceanic crust at shallow palaeodepths (~2.75 km) near to the ridge crest and, through time, subsiding below the CCD to their current depths of 4.3 km or more. Superimposed upon this subsidence-driven signal are relatively high-frequency, short-term fluctuations (~10–100s kyr), and long-term trends (1–10s myr) in the depth of the CCD at the basin-scale, which are driven by changes in regional to global-scale biogeochemical cycling (Pälike *et al.*, in prep.).

The effects of carbonate dissolution are most apparent in the oldest successions of Sites U1331 through U1333, as evidenced by low carbonate values, poor nannofossil preservation and the dominance of radiolarian ooze lithologies (Fig. 2; Pälike *et al.*, 2010). These observations are consistent with previous reconstructions of a very shallow Eocene CCD around 3–4 km depth. The most striking and sustained switch in the CCD is recorded close to the Eocene/Oligocene boundary, at Sites U1331 through U1334, and seen as a shift from radiolarian-dominated Eocene sediments to Oligocene nannofossil oozes. The depth transect afforded by these sites indicates a deepening of the CCD by ~1 km in less than 500 kyrs. The recovery of carbonate-rich Oligocene successions at all sites is evidence for a considerably deeper CCD (~4.5 km depth) throughout this time interval. For the younger, post-Eocene sites, the point at which the site drifted out of the palaeo-equatorial upwelling zone coincides with a transition to carbonate-poor or carbonate-free sediments.

Shipboard qualitative estimates of foraminifera and nannofossil preservation and abundance reveal a strong coupling between the preserved fossil record and the site's location relative to the CCD at any given time. They also highlight the very different sensitivities to dissolution across the fossil groups (Pälike *et al.*, 2010). Planktic foraminifera display the most dissolution-sensitive record of the documented microfossil groups, and are typically absent in sediments with carbonate contents less than 60–70 wt%CaCO₃. At the oldest site (Site U1331) they are almost entirely absent, appearing only where carbonate maxima occur in the Oligocene, middle Eocene and basal lower Eocene. At Site U1332 they are restricted to the carbonate-rich Oligocene nannofossil oozes. Only at Sites U1334 and U1335, where carbonate values remain at 80–90% or more for considerable thicknesses, are planktic foraminifera consistently recovered at high abundances and with good preservation.

Calcareous nannofossils and benthic foraminifera are less susceptible than planktic foraminifera to complete destruction by dissolution and their abundances closely track the presence/absence of carbonate in these sediments. This is not surprising given that coccoliths are, for the most part, the major carbonate contributors to these sediments. In general, however, the majority of nannofossil assemblages observed during Exp. 320 show some degree of modification by dissolution, with more robust taxa dominating most assemblages. Certain nannofossil taxa are especially sensitive to carbonate dissolution intensity. Holococcoliths, for example, are entirely absent except for one or two samples from Sites U1334–U1336, where the relatively robust *Zygrhablithus bijugatus* is recorded. *Helicosphaera* and *Pontosphaera* are typically absent at the older, deeper sites (Sites U1331–1333) and only consistently present in the younger sediments (Oligocene–Miocene) with high carbonate values, showing trends that are similar to the planktonic foraminifera. Similarly, Oligocene calcidiscids are only recorded consistently in the shallowest, best preserved sediments of Site U1334. The Eocene assemblages in general are strongly modified by preservation, typified by the absence of small coccoliths, concentration of dissolution-resistant discoasters and the loss of central structures in, for example, *Chiasmolithus*.

5. Stratigraphic range charts

Stratigraphic range charts are provided for Sites U1331 through U1334 (Charts 1–4). In most cases only data from Hole A at each site are included, though three or four holes were drilled at each site to provide complete composite sections. Revised composite depth scales for all sites are provided by Westerhold *et al.* (2011). The sampling resolution was dependent on the requirements of shipboard biostratigraphy. The amount of time spent on each sample is variable through the datasets, with most effort spent on core catcher (CC) samples, and section samples generally the focus for marker species logging. Most CC samples have been more thoroughly studied post-expedition, and post-expedition observations are indicated in bold on the charts. Sites U1333 and U1334, in particular, are currently being studied at higher resolution and will be the subject of additional biostratigraphic publications.

6. Systematic palaeontology

We provide images of the principal taxa from the IODP Exp. 320 Paleogene sites (U1331–1334) in 14 plates. The images are reproduced at constant magnification and a 2 μm scale bar is provided beside at least one of the images on each plate. The sample information is provided using standard IODP notation (Hole-Core-Section, depth in cm in section). For a number of key groups (e.g., reticulofenestrids, sphenoliths) we have included multiple images to illustrate the high degree of morphological variability present. All taxa figured are listed but taxonomic remarks are only provided where comment (stratigraphic or taxonomic) is necessary. Descriptive terminology follows the guidelines of Young *et al.* (1997). The higher taxonomy essentially follows the scheme for extant coccolithophores of Young *et*

[illegible]

Chart 1. Stratigraphic range chart for calcareous nannofossils from Hole U1331A. Biostratigraphic marker species and other notable occurrences are shaded, with darker shading at base and top horizons. Species abundance: A >10/field of view (FOV), C 1-10/FOV, F 1/2-10 FOV, R 1/11-100FOV, 1-5 total counts of very rare occurrences, ? questionable occurrence. Italics are used to indicate reworked occurrences. Nannofossil abundance:

A>10%, C 1-10%, F 0.1-1%, R<0.1%, B barren. Nannofossil preservation: G - good, M - moderate, P - poor. Nannofossil event notations are B = base, T = top, Tc = top common, Bc = base common. Nannofossil zones are after Martini (1971) and the timescale construction in general follows Pálke *et al.* (2010). Barren samples are shaded in black.

al. (2003) and, for the extinct taxa, the scheme of Young and Bown (1997) (see Dunkley Jones *et al.*, 2009 for further discussion). Informal groups have been used to indicate morphological affinity within high diversity genera, such as, *Reticulofenestra*, *Sphenolithus* and *Discoaster*. All new taxonomic names are Latin and the meaning and/or derivation is given in each case. Range information is given for stratigraphic distributions in the Exp. 320 sites. Morphometric data are given for all new taxa based on measurement from the type specimens and additional data is provided for the reticulofenestrids, sphenoliths and calcidiscids (Tables 1-3). Only those taxonomic references not listed in Perch-Nielsen (1985), Bown (1998) or Jordan *et al.* (2004) are included in the reference list. The following abbreviations are used: LM – light microscope, XPL cross-polarised light, PC – phase-contrast illumination, L – length, H – height, W – width, D – diameter. Type material and images are stored in the Department of Earth Sciences, University College London.

Order ISOCHRYSIDALES
Pascher, 1910

Pl. 1, figs 1-48; Pl. 2, 1-19

Remarks: The majority of the Exp. 320 nannofossil assemblages are dominated by reticulofenestrids (*Reticulofenestra*, *Cyclicargolithus*) that show a high degree of variability in size, outline, central area width and net type (Table 1). The established taxonomy for the Paleogene representatives of this group does not clearly accommodate or represent this variability, but this is equally true of younger representatives of the family (see, for example, discussion in Gallagher, 1989 and Young, 1990). Our classification herein applies widely-used species names and several new taxa, and places these within a framework of informal groups. We have not attempted a revision of the reticulofenestrids as a whole but instead highlight some

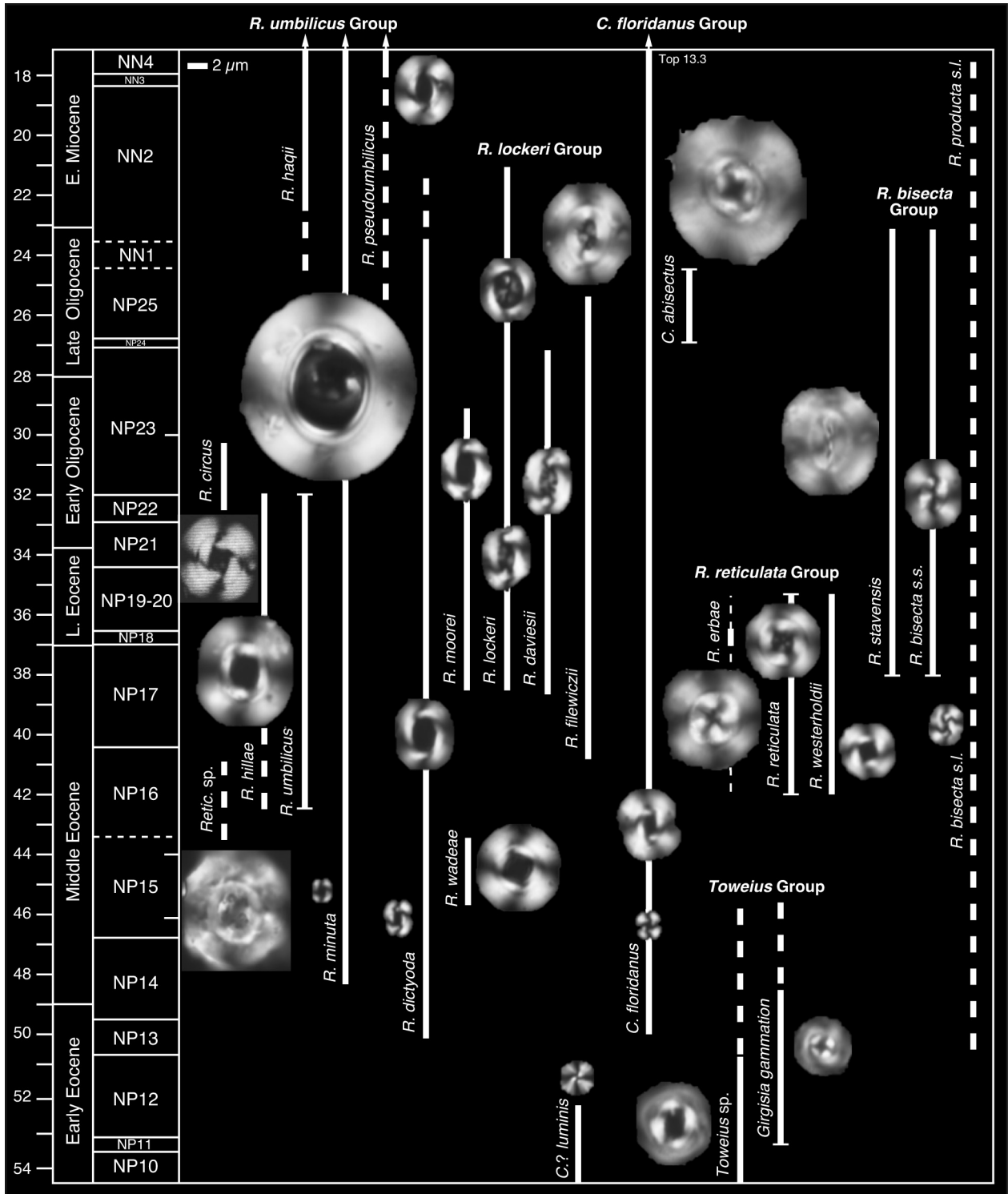


Figure 3. Stratigraphic distribution of Paleogene and early Neogene reticulofenestrids. The timescale is from Pälike *et al.* (2010). Dotted vertical lines are questionable stratigraphic ranges, horizontal bars indicate well constrained range base or top.

of the outstanding taxonomic issues. An overview of the stratigraphic distribution of Paleogene reticulofenestrids is given in Figure 3 and morphometric data is provided in Table 1. The informal groups are as follows:

1. *Reticulofenestra umbilicus* Group (common, middle Eocene-lower Oligocene) - typically elliptical outline and relatively open central area with thin, impercep-

tible net (non-birefringent or lost). There is a high degree of variability within this group, which was informally divided using simple coccolith length categories (see also Young, 1990). Forms with broadly elliptical to subcircular outlines and/or narrower central areas were in some cases difficult to distinguish from species of *Cyclicargolithus*.

Chart 2. Stratigraphic range chart for calcareous nannofossils from Hole U1332A. *See Chart 1 for further information.*

Chart 2. Continued

AGE	NANNOFOSSIL EVENTS	NANNOFOSSIL ZONE/SUBZONE	SAMPLE	DEPTH CSF-A (m)	PRESERVATION	ABUNDANCE	Sphenolithus fucaolithoides	Sphenolithus grandis	Sphenolithus intercalaris	Sphenolithus moniformis	Sphenolithus obtusus	Sphenolithus pearliae	Sphenolithus predistentus	Sphenolithus predistentus (large)	Sphenolithus pseudoradians	Sphenolithus radians	Sphenolithus richeri	Sphenolithus spinger	Sphenolithus strigosus	Sphenolithus tribulosus	Tetralithoides symeonidesii	Triquetrorhabdulus carinatus	Triquetrorhabdulus longus	Triquetrorhabdulus milovii	Umbilicosphaera bramlettei	caldispheres	diatoms	siliceous fragments	SPECIES RICHNESS	
Late Oligocene			U1332A-1H-CC	3.86	B																								0	
			U1332A-2H-CC	13.62	B																								0	
			U1332A-3H-1, 100	14.40	B																								0	
			U1332A-3H-3, 100	17.40	B																								0	
			U1332A-3H-4, 100	18.90	P	F																							3	
		T. T. carinatus	NN1	U1332A-3H-5, 100	20.40	P	A																							4
			U1332A-3H-6, 100	21.90	P	C																							3	
			U1332A-3H-7, 60	23.00	P	A																							7	
		?T. S. ciperensis		U1332A-3H-CC	23.51	P	A																							17
			U1332A-4H-1, 60	23.50	P	C																							2	
			U1332A-4H-2, 60	25.00	P	A																							5	
		X. T. longus/carinatus; T. C. abisectus	NP25	U1332A-4H-3, 60	26.50	M	A																							10
			U1332A-4H-5, 60	29.50	P	R																							5	
			U1332A-4H-6, 60	31.00	P	A																							14	
			U1332A-4H-7, 60	32.50	P	A																							11	
			U1332A-4H-CC	32.95	M-P	A																							18	
Early Oligocene			U1332A-5H-1, 80	33.20	M	A																							13	
			U1332A-5H-2, 80	34.70	M	A																							14	
			U1332A-5H-3, 80	36.20	M	A																							16	
			U1332A-5H-4, 80	37.70	M	A																							12	
			U1332A-5H-5, 80	39.20	M	A																							12	
			U1332A-5H-6, 80	40.70	M	A																							16	
			U1332A-5H-7, 80	42.20	M	A																							16	
		B. C. abisectus		U1332A-5H-CC	42.47	M	A																						31	
			U1332A-6H-1, 70	42.60	M	A																							13	
		B. S. ciperensis		U1332A-6H-3, 70	45.60	M	A																						16	
			U1332A-6H-4, 70	47.10	M	A																							8	
			U1332A-6H-5, 70	48.60	M	A																							13	
			U1332A-6H-6, 70	50.10	M	A																							14	
			U1332A-6H-7, 70	51.60	P	A																							12	
			U1332A-6H-CC	51.97	M-P	A																							21	
			U1332A-7H-3, 80	52.20	M	A																							12	
			U1332A-7H-5, 80	58.20	M	A																							11	
			U1332A-7H-6, 80	59.70	M	D																							11	
		T. R. umbilicus		U1332A-7H-7, 80	61.20	M	A																						13	
			NP22	U1332A-7H-CC	61.49	M	A																						27	
			U1332A-8H-2, 50	62.90	M	A																							2	
			U1332A-8H-3, 50	64.40	M	A																							2	
			U1332A-8H-4, 50	65.90	M	A																							13	
		T. C. formosus		U1332A-8H-5, 50	67.40	M	A																						3	
			U1332A-8H-6, 50	68.90	M	A																							14	
			U1332A-8H-7, 50	70.40	M	A																							2	
			U1332A-8H-CC	71.00	M	A																							26	
			U1332A-9H-1 base	71.90	M-P	A																							11	
			U1332A-9H-3 base	74.90	M	D																		</						

2. *Reticulofenestra lockeri* Group (common, upper Eocene-upper Oligocene) - elliptical outline and relatively open central area with robust, visible net (birefringent).
3. *Reticulofenestra reticulata* Group (common, middle-upper Eocene) - typically circular outline and relatively narrow circular central area with robust, visible net (birefringent). This group includes the only strictly circular Paleogene reticulofenestrids but some smaller forms had imperceptible (or lost) nets and there is some evidence of transitional subcircularity.
4. *Reticulofenestra bisecta* Group (common, upper Eocene-lower Oligocene) - elliptical outline and central area closed by very robust, conspicuous distal 'plug' (birefringent). As defined this group is essentially restricted to the Paleogene.
5. *Cyclicargolithus floridanus* (common in the Eocene and dominant, lower Oligocene-lower Miocene) - subcircular to broadly elliptical outline and narrow central area with thin, imperceptible net (non-birefringent or lost).

Group 3 broadly, but not completely, correlates with the general usage of the genus *Criboecentrum* Perch-Nielsen, 1971 and Group 4 with the genus *Dictyococcites* Black, 1967. These generic names are not applied here, because we currently lack a good understanding of the phylogenetic relationships between these reticulofenestrids.

6.1.1. *Reticulofenestra umbilicus* Group

Reticulofenestra dictyoda
(Deflandre in Deflandre & Fert, 1954)
Stradner in Stradner & Edwards, 1968
Pl. 1, figs 2-6, 9-10.

Remarks: Small to very large (3-14 μm), elliptical reticulofenestrids with open central area. There is a great deal of morphological variability within this group, including degree of ellipticity/circularity, size of central area and width of tube cycle. A broad species concept is applied here.

Reticulofenestra circus? de Kaenel & Villa, 1996

Pl. 1, figs 19-20

Remarks: Not consistently logged herein and close to the applied species concept of *Reticulofenestra hillae* (see below), but should be subcircular. The specimens illustrated here have axial ratios of 1.12, which is strictly broadly elliptical (see Young *et al.*, 1997 for outline definitions).

Species	Pl., fig. number	L	W	L/W	outline
<i>R. minuta</i>	Pl. 1, fig. 1	2.6	2.0	1.30	normally elliptical
<i>R. minuta</i>	Pl. 1, fig. 8	2.4	1.8	1.33	normally elliptical
<i>R. minuta</i>	Pl. 1, fig. 8	2.8	2.0	1.40	normally elliptical
<i>R. dictyoda</i>	Pl. 1, fig. 2	4.0	2.9	1.38	normally elliptical
<i>R. dictyoda</i>	Pl. 1, fig. 3	6.6	5.2	1.27	normally elliptical
<i>R. dictyoda</i>	Pl. 1, fig. 4	7.6	6.3	1.21	broadly elliptical
<i>R. dictyoda</i>	Pl. 1, fig. 5	12.5	10.4	1.20	broadly elliptical
<i>R. dictyoda</i>	Pl. 1, fig. 6	12.9	10.9	1.18	broadly elliptical
<i>R. umbilica</i>	Pl. 1, fig. 7	19.1	17.5	1.09	subcircular
<i>R. dictyoda</i>	Pl. 1, fig. 9	8.5	7.0	1.21	broadly elliptical
<i>R. dictyoda</i>	Pl. 1, fig. 10	5.7	4.7	1.21	broadly elliptical
<i>R. pseudoumbilicus</i>	Pl. 1, fig. 11	7.3	6.1	1.20	broadly elliptical
<i>R. pseudoumbilicus</i>	Pl. 1, fig. 12	9.7	7.8	1.24	broadly elliptical
<i>R. moorei</i>	Pl. 1, fig. 13	6.2	4.5	1.38	normally elliptical
<i>R. moorei</i>	Pl. 1, fig. 14	5.8	4.3	1.35	normally elliptical
<i>R. moorei</i>	Pl. 1, fig. 15	6.8	5.4	1.26	normally elliptical
<i>R. moorei</i>	Pl. 1, fig. 16	6.1	4.4	1.39	normally elliptical
<i>R. moorei</i>	Pl. 1, fig. 17	6.9	5.4	1.28	normally elliptical
<i>R. wadeae</i>	Pl. 1, fig. 18	10.0	8.9	1.12	broadly elliptical
<i>R. circus</i>	Pl. 1, fig. 19	9.1	8.1	1.12	broadly elliptical
<i>R. circus</i>	Pl. 1, fig. 20	11.1	9.9	1.12	broadly elliptical
<i>R. hillae</i>	Pl. 1, fig. 21	9.2	7.9	1.16	broadly elliptical
<i>R. hillae</i>	Pl. 1, fig. 22	11.7	10.1	1.16	broadly elliptical
<i>R. hillae</i>	Pl. 1, fig. 23	11.6	9.7	1.20	broadly elliptical
<i>R. hillae</i>	Pl. 1, fig. 24	12.7	11.3	1.12	broadly elliptical
<i>R. lockeri</i>	Pl. 1, fig. 25	6.9	5.2	1.33	normally elliptical
<i>R. lockeri</i>	Pl. 1, fig. 26	8.2	6.8	1.21	broadly elliptical
<i>R. lockeri</i>	Pl. 1, fig. 27	7.8	6.2	1.26	normally elliptical
<i>R. cf. R. lockeri</i>	Pl. 1, fig. 28	6.9	6.0	1.15	broadly elliptical
<i>R. daviesii</i>	Pl. 1, fig. 29	6.0	4.5	1.33	normally elliptical
<i>R. daviesii</i>	Pl. 1, fig. 30	7.1	5.2	1.37	normally elliptical
<i>R. cf. R. daviesii</i>	Pl. 1, fig. 36	5.7	4.5	1.27	normally elliptical
<i>R. filewiczii</i>	Pl. 1, fig. 31	7.9	6.4	1.23	broadly elliptical
<i>R. filewiczii</i>	Pl. 1, fig. 32	7.4	6.1	1.21	broadly elliptical
<i>R. filewiczii</i>	Pl. 1, fig. 33	11.1	9.2	1.21	broadly elliptical
<i>R. filewiczii</i>	Pl. 1, fig. 34	12.6	11.2	1.13	broadly elliptical
<i>R. filewiczii</i>	Pl. 1, fig. 35	12.3	11.4	1.08	subcircular
<i>R. westerholdii</i>	Pl. 1, fig. 37	5.5	5.5	1.00	circular
<i>R. westerholdii</i>	Pl. 1, fig. 38	5.9	5.9	1.00	circular
<i>R. westerholdii</i>	Pl. 1, fig. 39	6.9	6.8	1.01	circular
<i>R. cf. R. westerholdii</i>	Pl. 1, fig. 40	6.3	5.8	1.09	subcircular
<i>R. cf. R. westerholdii</i>	Pl. 1, fig. 41	7.0	6.0	1.17	broadly elliptical
<i>R. cf. R. westerholdii</i>	Pl. 1, fig. 42	7.7	6.6	1.17	broadly elliptical
<i>R. cf. R. westerholdii</i>	Pl. 1, fig. 43	9.2	8.1	1.14	broadly elliptical
<i>R. reticulata</i>	Pl. 1, fig. 44	8.1	8.0	1.01	circular
<i>R. reticulata</i>	Pl. 1, fig. 45	9.3	9.2	1.01	circular
<i>R. reticulata</i>	Pl. 1, fig. 46	10.2	10.1	1.01	circular
<i>R. erbae</i>	Pl. 1, fig. 47	10.6	10.2	1.04	subcircular
<i>R. cf. R. reticulata</i>	Pl. 1, fig. 48	10.3	8.2	1.26	normally elliptical
<i>R. cf. R. reticulata</i>	Pl. 2, fig. 1	11.0	10.4	1.06	subcircular
<i>R. cf. R. reticulata</i>	Pl. 2, fig. 2	9.0	7.8	1.15	broadly elliptical
<i>R. cf. R. reticulata</i>	Pl. 2, fig. 3	10.0	9.0	1.11	broadly elliptical
<i>C. cf. C. floridanus</i>	Pl. 2, fig. 4	10.2	9.2	1.11	broadly elliptical
<i>C. cf. C. abisectus</i>	Pl. 2, fig. 5	12.2	11.2	1.09	subcircular
<i>C. cf. C. abisectus</i>	Pl. 2, fig. 6	11.8	10.5	1.12	broadly elliptical
<i>C. floridanus</i>	Pl. 2, fig. 7	2.8	2.6	1.08	subcircular
<i>C. floridanus</i>	Pl. 2, fig. 8	5.7	5.2	1.10	broadly elliptical
<i>C. floridanus</i>	Pl. 2, fig. 9	7.7	6.5	1.18	broadly elliptical
<i>C. floridanus</i>	Pl. 2, fig. 10	9.7	8.8	1.10	broadly elliptical
<i>C. floridanus</i>	Pl. 2, fig. 11	10.9	9.9	1.10	broadly elliptical
<i>C. abisectus</i>	Pl. 2, fig. 18	15.4	13.5	1.14	broadly elliptical
<i>R. bisecta</i>	Pl. 2, fig. 13	4.2	3.5	1.20	broadly elliptical
<i>R. bisecta</i>	Pl. 2, fig. 14	6.9	5.3	1.30	normally elliptical
<i>R. bisecta</i>	Pl. 2, fig. 15	7.3	6.1	1.20	broadly elliptical
<i>R. stavensis</i>	Pl. 2, fig. 16	11.5	10.0	1.15	broadly elliptical
<i>R. stavensis</i>	Pl. 2, fig. 17	17.2	15.2	1.13	broadly elliptical

Table 1. Morphometric data (L, W, L/W axial ratio) and descriptive shape terms for the illustrated reticulofenestrids. The descriptive terms and definitions are slightly modified after Young *et al.* (1997): circular 1.00-1.03, subcircular 1.04-1.09, broadly elliptical 1.10-1.25, narrowly elliptical 1.26-1.45.

low), but should be subcircular. The specimens illustrated here have axial ratios of 1.12, which is strictly broadly elliptical (see Young *et al.*, 1997 for outline definitions).

Chart 3. Stratigraphic range chart for calcareous nannofossils from Hole U1333A. *See Chart 1 for further information.*

Chart 3. *Continued*

Chart 3. *Continued*

Chart 3. *Continued*

Reticulofenestra hillae Bukry & Percival, 1971

Pl. 1, figs 21-24

Remarks: Used here for large ($\sim 9\mu\text{m}$), broadly elliptical reticulofenestrids with narrow central area that can be distinctly quadrate or lens-shaped. This includes coccoliths that are smaller than those of the original type material (14–20 μm). This is similar to the species concept of *Reticulofenestra circus* de Kaenel & Villa, 1996 (described as subcircular, 8–10 μm) and *Reticulofenestra circus* var. *lata* Maiorano, 2006 (12–14 μm), but the specimens from Exp. 320 are broadly elliptical and most like the holotype of *R. hillae*. **Occurrence:** Particularly conspicuous in the Eocene/Oligocene boundary interval and lower Oligocene (Zones NP19/20–NP22) but also present in the Eocene (Zones NP17–NP19/20); IODP Site U1334. *R. circus* is documented from Zones NP22–NP23 (de Kaenel & Villa, 1996; Maiorano, 2006).

Reticulofenestra minuta Roth, 1970

Pl. 1, figs 1, 8. **Remarks:** Small ($<3\mu\text{m}$), elliptical with open central area.

Reticulofenestra moorei sp. nov.

Pl. 1, figs 13-17

Derivation of name: Named after Ted Moore (University of Michigan, USA), Exp. 320 shipboard scientist, micropalaeontologist and palaeoceanographer. **Diagnosis:** Normally elliptical reticulofenestrid with relatively wide central area and an net that is faintly visible or imperceptible. **Differentiation:** Distinguished from other *R. umbilicus* group and *R. lockeri* group coccoliths by narrower shape (axial ratio ~ 1.26 – 1.40 ; Table 1). **Dimensions:** Holotype L = 6.8 μm (Paratype L = 6.2 μm). **Holotype:** Pl.1, fig.15. **Paratype:** Pl.1, figs 13. **Type locality:** IODP Hole U1333A, Pacific Ocean. **Type level:** Oligocene, Sample U1333A-11X-CC (Zone NP22). **Occurrence:** Zone NP17–Zone NP23; IODP Sites U1333 (NP21–NP23), 1334. Particularly common in the Eocene/Oligocene boundary interval and lower Oligocene (NP19/20–NP22).

Reticulofenestra pseudumbilicus (Gartner, 1967)

Gartner, 1969

Pl. 1, figs 11-12

Remarks: The differentiation between Paleogene *R. umbilicus* Group coccoliths and Neogene *Reticulofenestra pseudumbilicus* is highly problematic, and beyond the scope of this paper. Suffice to say, the two groups overlap morphologically and the species concepts are essentially stratigraphy dependent.

Reticulofenestra umbilicus (Levin, 1965)

Martini & Ritzkowski, 1968

Pl. 1, fig. 7

Reticulofenestra wadeae Bown, 2005

Pl. 1, fig. 18

6.1.2. *Reticulofenestra lockeri* Group

Reticulofenestra daviesii (Haq 1968) Haq, 1971

Pl. 1, figs 29-30.

Remarks: Usually applied to forms that possess a visible central net with an outer cycle of pores, but appears to

intergrade with *R. lockeri* type coccoliths with nets without visible pores. The appearance of these taxa may be affected by different preservation states.

Reticulofenestra cf. *R. daviesii* (Haq 1968) Haq, 1971

Pl. 1, fig. 36.

Like *R. daviesii* but the central area is very narrow.

Reticulofenestra filewiczii (Wise & Wiegand in Wise, 1983) Dunkley Jones *et al.*, 2009

Pl. 1, figs 31-35.

Remarks: Broadly elliptical with a narrow central area and birefringent net.

Reticulofenestra lockeri Müller, 1970

Pl. 1, figs 25-27

Reticulofenestra cf. *R. lockeri* Müller, 1970

Pl. 1, fig. 28.

Remarks: Like *R. lockeri* but with relatively wider central area.

6.1.3. *Reticulofenestra reticulata* Group

Reticulofenestra erbae Fornaciari *et al.*, 2010

Pl. 1, fig. 47.

Remarks: Like *R. reticulata* but with a closed central area. **Occurrence:** Zone NP19/20; Site U1334; NP17–NP19, Fornaciari *et al.* (2010).

Reticulofenestra reticulata (Gartner & Smith, 1967)

Roth & Thierstein, 1972

Pl. 1, figs 44-46

Remarks: Medium to large (~ 8 – $12\mu\text{m}$), circular reticulofenestrid with narrow central area crossed by a distinctive, robust, visible net. Subcircular to elliptical forms have also been observed (Pl. 1., fig. 48; Pl. 2, figs 1-3) and may intergrade with the *R. filewiczii* morphotype. **Occurrence:** Zone NP17–Zone NP19/20; IODP Sites U1331, 1333-1334.

Reticulofenestra cf. *R. reticulata*

(Gartner & Smith, 1967) Roth & Thierstein, 1972

Pl. 1, figs 48; Pl. 2, figs 1-3.

Remarks: Like *R. reticulata* but subcircular to broadly elliptical. These morphotypes are similar to *R. filewiczii*. **Occurrence:** Zone NP19/20; Site U1334.

Reticulofenestra westerholdii sp. nov.

Pl. 1, figs 37-39.

Derivation of name: Named after Thomas Westerhold (University of Bremen, Germany), Exp. 320 shipboard scientist, stratigrapher and palaeoceanographer. **Diagnosis:** Medium sized (5–8 μm), circular reticulofenestrid with open central area (similar in width to, or slightly narrower than, the rim width) but no perceptible net. Subcircular to broadly elliptical forms are rarely observed and distinguished as *R. cf. R. westerholdii* (Pl. 1. figs 40-43). **Differentiation:** Distinguished from *R. reticulata* by the smaller size, narrower tube, proportionally wider central area and absence of visible net. Distinguished from *C. floridanus* by the circular outline, wider central area and low tube cycle. **Dimensions:** Holotype L = 6.9 μm (Paratype L =

AGE	NANNOFOSSIL EVENTS	NANNOFOSSIL ZONE/SUBZONE	SAMPLE	DEPTH CSF-A (m)	OFFSET	DEPTH CCSF-A (m)	PRESERVATION	ABUNDANCE	Blackites spinosus	Blackites tenuis	Blackites bases	Blackites spines	Bramletteius serraculoides	Calcidiscus bicircus	Calcidiscus? detecta	Calcidiscus? detecta (subcirc.)	Calcidiscus? edgarae	Calcidiscus leptoporus	Calcidiscus pacificanus	Calcidiscus pataecus <5µm	Calcidiscus pataecus >5µm	Calcidiscus pataecus subcirc. >5µm	Calcidiscus premaxillaris	Calcidiscus protoannulus	Calcidiscus tropicus	Calciolenia fossilis	Campylospira dela	Chiasmolithus altus	Chiasmolithus grandis	Chiasmolithus nitidus		
Early Miocene		B	U1334A-1H-CC	8.19	0.00	8.19	B	B																								
		m-INN6	U1334A-2H-CC	18.11	0.87	18.98	M	A																								
	B/T S. heteromorphus	uNN4-5	U1334A-3H-CC	27.65	1.97	29.62	M	A																								
		?	U1334A-4H-CC	37.18	3.48	40.66	P	R																								
	T. T. carinatus		U1334A-5H-CC	46.78	4.77	51.55	M	A																								
	B. S. belemnus		U1334A-6H-CC	56.20	6.93	63.13	M	A																								
	T. S. disbelemnus		U1334A-7H-CC	65.66	7.42	73.08	M-G	A																								
			U1334A-8H-CC	75.06	9.06	84.12	M-G	A																								
			U1334A-9H-2, 110	77.30	11.22	88.52	M	A																								
			U1334A-9H-3, 20	77.90	11.22	89.12	M	A																								
Late Oligocene		NN2	U1334A-9H-4, 100	80.20	11.22	91.42	M-G	A																								
			U1334A-9H-6, 70	82.90	11.22	94.12	M-G	A																								
	B. S. disbelemnus		U1334A-9H-7, 30	84.00	11.22	95.22	M	A																								
	B. D. druggii		U1334A-9H-CC	84.74	11.22	95.96	P-M	A																								
			U1334A-10H-3, 90	88.10	11.31	99.41	P-M	A																								
			U1334A-10H-6, 90	92.60	11.31	103.91	M	A																								
			U1334A-10H-7, 30	93.50	11.31	104.81	M	A																								
			U1334A-10H-CC	93.95	11.31	105.26	M-G	A																								
	T. S. delphix		U1334A-11H-1, 20	94.70	12.92	107.62	M-G	A																								
	B. S. delphix		U1334A-11H-2, 20	96.20	12.92	109.12	M	A																								
Early Eocene		NN1	U1334A-11H-3, 20	96.90	12.92	109.82	M	A																								
			U1334A-11H-6, 20	101.50	12.92	114.42	M	A																								
			U1334A-11H-CC	103.75	12.92	116.67	M	A																								
			U1334A-12H-2, 70	105.40	14.15	119.55	P-M	A																								
			U1334A-12H-4, 70	108.40	14.15	122.55	P-M	A																								
			U1334A-12H-6, 70	111.40	14.15	125.55	M	A																								
			U1334A-12H-7, 30	112.27	14.15	126.42	P-M	A																								
			U1334A-12H-CC	112.58	14.15	126.73	M	A																								
	T. S. ciproensis		U1334A-13H-1, 45	113.15	15.44	128.59	M	A																								
	T. C. abisectus		U1334A-13H-2, 45	113.65	15.44	129.09	M	A																								
Middle Eocene		NP25	U1334A-13H-4, 10	116.30	15.44	131.74	M-G	A																								
			U1334A-13H-6, 45	119.65	15.44	135.09	M	A																								
			U1334A-13H-CC	122.55	15.44	137.99	M-G	A																								
			U1334A-14H-2, 40	124.10	16.93	141.03	M	A																								
			U1334A-14H-4, 40	127.10	16.93	144.03	P-M	F																								
			U1334A-14H-6, 40	130.10	16.93	147.03	M	A																								
			U1334A-14H-CC	131.96	16.93	148.89	P-M	A																								
			U1334A-15H-2, 110	134.30	18.86	153.16	M-G	A																								
			U1334A-15H-4, 110	137.30	18.86	156.16	M	A																								
			U1334A-15H-6, 40	139.60	18.86	158.46	P-M	A																								
Late Eocene		NP24	U1334A-15H-CC	141.20	18.86	160.06	M-G	A																								
	B. S. ciproensis/T. S. predistentus		U1334A-16H-2, 110	143.80	20.56	164.36	M-G	A																								
			U1334A-16H-4, 110	146.80	20.56	167.36	M-G	A																								
			U1334A-16H-6, 40	149.10	20.56	169.66	M-G	A																								
			U1334A-16H-CC	149.57	20.56	170.13	M-G	A																								
			U1334A-17H-2, 60	152.80	23.22	176.02	M-G	A																								
			U1334A-17H-4, 60	155.80	23.22	179.02	M	A																								
			U1334A-17H-6, 60	158.80	23.22	182.02	M	A																								
			U1334A-17H-CC	159.97	23.22	183.19	G	A																								
			U1334A-18H-3, 60				M	A																								
Early Eocene	B. C. abisectus		U1334A-18H-CC	170.17	24.10	194.27	M-G	A																								
			U1334A-19H-3, 70				M-G	A																								
	B. S. ciproensis		U1334A-19H-CC	178.49	26.42	204.91	M-G	A																								
	?B. S. distentus		U1334A-20H-CC	188.63	40.46	229.09	M-G	A																								
			U1334A-21H-CC	198.48	41.16	239.64	M	A																								
			U1334A-22H-2, 70	200.40	42.46	242.86	M	A																								
			U1334A-22H-4, 70	203.40	42.46	245.86	M	A																								
			U1334A-22H-6, 30	206.00	42.46	248.46	P-M	A																								
			U1334A-22H-CC	206.86	42.46	249.32	M	A																								
			U1334A-23H-3, 70				P-M	A																								
Middle Eocene		NP23	U1334A-23X-CC	216.17	44.72	260.89	M	A																								

Chart 4. *Continued*

Chart 4. *Continued*

[illegible]Chart 4. *Continued*

Chart 4. *Continued*

5.9 μm). **Holotype:** Pl.1, fig.39. **Paratype:** Pl.1, figs 38. **Type locality:** IODP Hole U1334A, Pacific Ocean. **Type level:** Upper Eocene, Sample U1334A-28H-CC (Zone NP19/20). **Occurrence:** Can be common to abundant. Zone NP16-Zone NP19/20; IODP Sites U1331-1334.

Reticulofenestra cf. *R. westerholdii* sp. nov.

Pl. 1, figs 40-43.

Remarks: Like *R. westerholdii* but subcircular to broadly elliptical. **Occurrence:** Zone NP19/20; Site U1334.

6.1.4. *Cyclicargolithus floridanus* Group

Cyclicargolithus abisectus

(Roth & Hay, in Hay *et al.*, 1967) Bukry, 1971

Pl. 2, fig. 18.

Remarks: Large *Cyclicargolithus* (>11.0 μm) with relatively consistent stratigraphic range in the equatorial Pacific (NP24-NP25), but similar morphotypes do occur earlier (Pl. 2, figs 4-5) and morphometric studies suggests the 11 μm cut-off is rather arbitrary (Firth, 1992; Olafsson, 1992).

Cyclicargolithus cf. *C. abisectus*

(Roth & Hay, in Hay *et al.*, 1967) Bukry, 1971

Pl. 2, fig. 4-5.

Remarks: Large subcircular to broadly elliptical reticulofenestrids with conspicuous tube cycle and narrow central area. Similar to upper Eocene *Reticulofenestra* cf. *R. reticulata* and upper Oligocene *Cyclicargolithus abisectus*. They appear to have slightly lower tube cycles than the latter and so are differentiated here, although the difference is subtle. **Occurrence:** Zone NP21-lower NP22; Sites U1333, 1334.

Cyclicargolithus floridanus

(Roth & Hay, in Hay *et al.*, 1967) Bukry, 1971

Pl. 2, figs 6-12

Cyclicargolithus? luminis (Sullivan, 1965) Bukry, 1971

Pl. 2, fig. 19

6.1.5. *Reticulofenestra bisecta* Group

Reticulofenestra bisecta (Hay *et al.*, 1966) Roth, 1970

Pl. 2, figs 13-15.

Remarks: The holotype length of *R. bisecta* is 8 μm and we use the species name here for specimens <10 μm in length. It should be noted that this species concept, based upon size ranges, is applied differently by some authors (see Young, 1998, p. 248).

Reticulofenestra stavensis

(Levin & Joerger, 1967) Varol, 1989

Pl. 2, figs 16-17.

Remarks: The holotype size of *R. stavensis* is 14 μm and we use the species here for the size range 10-20 μm .

Family **PRINSIACEAE** Hay & Mohler, 1967 emend.

Young & Bown, 1997

Genus *Towieus* Hay & Mohler, 1967

Pl. 2, figs 20-25.

Remarks: *Towieus* was one of the dominant placolith groups of the late Paleocene to early Eocene but went into decline broadly coincident with the appearance and rise to dominance of the reticulofenestrid group (early Eocene, zones NP12-13) (e.g., Agnini *et al.* 2006). The extinction levels of the youngest *Towieus* species are not particularly well constrained, however, Bralower and Mutterlose (1995) report the top of *Towieus* spp. in Zone NP12 and *Girgisia gammation* in Zone NP14 at ODP Site 865, and Perch-Nielsen (1985) reports *T. callosus* and *G. gammation* into Zone NP15. The species *G. gammation* has been placed both in *Towieus* and a separate genus *Girgisia* and ranges from Zone NP11-NP15. Relatively common *Towieus* coccoliths are present in the basal sediments at Site U1331 (Zone NP12/NP13 transition), including *T. pertusus*, *T. callosus* and *G. gammation*-like forms, and Site U1333 (Zone NP15), including *T. pertusus* and *G. gammation*-like forms, but are absent in the highly dissolved basal sediments of Site U1332 (Zone NP14), which contain only discoasters.

Towieus callosus Perch-Nielsen, 1971

Pl. 2, fig. 22

Girgisia gammation? (Bramlette & Sullivan, 1961)

Varol, 1989

Pl. 2, figs 23-25

Remarks: The specimens seen at Site U1331 were identified as *G. gammation* but they do not show the distinctive curving extinction lines that characterise the species. This is probably due to etching of the coccoliths, which may also lead to enlargement of the central area and loss of the tube cycle.

Towieus pertusus (Sullivan, 1965) Romein, 1979

Pl. 2, fig. 21

Order COCCOSPHERALES Haeckel, 1894 emend.

Young & Bown, 1997

Family **CALCIDISCACEAE** Young & Bown, 1997

Pl. 2, figs 26-49; Pl. 3; Pl. 4, 1-11

Remarks: The Exp. 320 calcidiscid and calcidiscid-like coccoliths are divided here into three informal groups:

1. Paleogene calcidiscid Group – a morphologically diverse group of elliptical to circular placoliths with only some taxa having proven calcidiscid morphology, while most await more detailed morphological analysis (Bown *et al.*, 2007).
2. *Calcidiscus leptoporus* Group - predominantly Neogene to Modern group with early forms recorded in the Oligocene in the Exp. 320 material.
3. Other calcidiscids – includes the predominantly Neogene to Modern forms not included in the *C. leptoporus* Group.

6.1.6. Paleogene calcidiscid Group

Calcidiscus? detectus

(de Kaenel & Villa, 1996) comb. nov.

Basionym: *Ericsonia detecta* (de Kaenel & Villa, 1996), p. 125, pl. 4, figs 1-3. ODP Sci. Res., 149: 79-145.

Pl. 2, figs 26-35.

Species	Pl., fig. number	L	W	L/W	CA W	Rim W	Rim W/CA W	Rim W/W	outline
<i>C. ? detectus</i>	Pl. 2, fig. 26	5.4	4.2	1.29	1.60	1.10	0.69	0.26	normally elliptical
<i>C. ? detectus</i>	Pl. 2, fig. 28	7.9	6.0	1.32	2.50	1.30	0.52	0.22	normally elliptical
<i>C. ? detectus</i>	Pl. 2, fig. 30	7.6	6.1	1.25	2.80	1.90	0.68	0.31	broadly elliptical
<i>C. ? detectus</i>	Pl. 2, fig. 32	8.4	7.0	1.20	2.90	1.90	0.66	0.27	broadly elliptical
<i>C. ? detectus</i>	Pl. 2, fig. 34	6.1	5.6	1.09	2.30	1.60	0.70	0.29	subcircular
<i>C. ? edgariae</i>	Pl. 2, fig. 36	5.5	4.5	1.22	1.40	1.40	1.00	0.31	broadly elliptical
<i>C. ? edgariae</i>	Pl. 2, fig. 38	5.6	4.5	1.24	1.40	1.50	1.07	0.33	broadly elliptical
<i>C. ? edgariae</i>	Pl. 2, fig. 40	7.6	6.4	1.19	1.80	2.10	1.17	0.33	broadly elliptical
<i>C. ? edgariae</i>	Pl. 2, fig. 43	7.8	6.5	1.20	1.87	2.31	1.24	0.36	broadly elliptical
<i>C. ? edgariae</i>	Pl. 2, fig. 44	7.2	6.5	1.11	1.90	2.30	1.21	0.35	broadly elliptical
<i>C. ? edgariae</i>	Pl. 2, fig. 47	8.9	7.3	1.22	1.90	2.60	1.37	0.36	broadly elliptical
<i>C. ? edgariae</i>	Pl. 2, fig. 49	9.1	7.9	1.15	2.30	2.80	1.22	0.35	broadly elliptical
<i>C. ? kamikurii</i>	Pl. 3, fig. 2	9.2	8.4	1.10	2.00	3.40	1.70	0.40	broadly elliptical
<i>C. ? kamikurii</i>	Pl. 3, fig. 4	9.0	8.2	1.10	1.80	2.90	1.61	0.35	broadly elliptical
<i>C. ? kamikurii</i>	Pl. 3, fig. 6	7.8	6.9	1.13	1.40	2.60	1.86	0.38	broadly elliptical
<i>P. larvalis</i>	Pl. 3, fig. 8	7.0	7.0	1.00	0.80	3.10	3.88	0.44	circular
<i>P. larvalis</i>	Pl. 3, fig. 9	9.9	9.9	1.00	1.30	5.10	3.92	0.52	circular
<i>P. gibbsiae</i>	Pl. 3, fig. 11	8.3	8.3	1.00	1.90	3.10	1.63	0.37	circular
<i>P. gibbsiae</i>	Pl. 3, fig. 14	8.8	8.8	1.00	2.40	3.20	1.33	0.36	circular
<i>P. gibbsiae</i>	Pl. 3, fig. 16	9.0	9.0	1.00	2.60	3.50	1.35	0.39	circular

Table 2. Morphometric data (L, W, L/W axial ratio, central area CA width) and descriptive shape terms for the illustrated calcidiscids. For descriptive terms and definitions see Table 1.

Remarks: Medium to large (~5-9 μ m), elliptical placolith coccoliths with narrow bicyclic rim (in XPL) and wide, apparently vacant, central area. The rim width is around half that of the central area (rim width/central area width: 0.5-0.7; Table 2). **Differentiation:** Similar to *Calcidiscus protoannulus* but strongly elliptical, and to *Calcidiscus? edgariae* sp. nov., but with narrower shields. **Remarks:** Only consistently present in the site with best Oligocene preservation (Site U1334), suggesting it is susceptible to dissolution. **Occurrence:** Zones NP22-25 (single occurrence in Zone NP21, one questionable Zone NP17 occurrence); Sites U1333, U1334. Present in very few samples at U1333 (Zones NP22-23) and absent at U1332.

Calcidiscus? edgariae sp. nov.
Pl. 2, figs 36-49

Derivation of name: Named after Kirsty Edgar (University of Cardiff, UK), Exp. 320 shipboard scientist, micropalaeontologist and palaeoceanographer. **Diagnosis:** Medium to large (~5-10 μ m), broadly elliptical placolith coccoliths with broad bicyclic rim (in XPL) and vacant central area. The rim width is similar to, or slightly greater than, that of the central area (rim width/central area width: 1.0-1.4; Table 2). **Differentiation:** Distinguished from *Calcidiscus? detectus* by the broader rim and relatively narrower central area. **Remarks:** Only consistently present in the site with best Oligocene preservation (Site U1334), suggesting it is susceptible to dissolution. **Dimensions:** Holotype L = 8.9 μ m (Paratypes L = 5.5, 7.8 μ m). **Holotype:** Pl.2, fig.46. **Paratype:** Pl.2, figs 36, 42. **Type locality:** IODP Hole U1334A, Pacific Ocean. **Type level:** Oligocene, Sample U1334A-19H-CC (Zone NP23). **Occurrence:** Zone NP23-Zone NP25 (single occurrence in Zone NP21); IODP Sites U1333, 1334. Present in very few samples at U1333 (Zone NP23) and absent at U1332.

Calcidiscus? kamikurii sp. nov.
Pl. 3, figs 1-6

Derivation of name: Named after Shin-ichi Kamikuri (Hokkaido University, Japan), IODP Expedition 320 shipboard scientist and micropalaeontologist. **Diagnosis:** Medium to large (~7-10 μ m), broadly elliptical placolith coccoliths with broad bicyclic rim (in XPL) and vacant, narrow central area. The rim width is greater than the central area width (rim width/central area width: 1.6-1.9; Table 2). **Differentiation:** Similar to *Calcidiscus? edgariae* but more broadly elliptical with relatively broader rim and narrower central area. *Pedinocyclus larvalis* and *P. okayi* (Pl. 3, figs 7-16) have elements joined along sutures with strong obliquity. **Dimensions:** L = 9.2 μ m (Paratype L = 9.0 μ m). **Holotype:** Pl.3, fig.1. **Paratype:** Pl.3, fig.3. **Type locality:** IODP Hole U1334A, Pacific Ocean. **Type level:** Oligocene, Sample U1334A-20H-CC (Zone NP23). **Occurrence:** Zone NP23-Zone NP24; IODP Site U1334.

Calcidiscus? bicircus Bown, 2005

Pl. 4, fig. 7

Calcidiscus? henrikseniae Bown, 2005

Pl. 4, fig. 8

Calcidiscus? pacificanus (Bukry, 1971) Varol, 1989

Pl. 4, fig. 9

Calcidiscus protoannulus

(Gartner, 1971) Loeblich & Tappan, 1978

Pl. 3, figs 19-20

Coronocyclus nitescens

(Kamptner 1963) Bramlette & Wilcoxon 1967

Pl. 3, figs 23-24

Umbilicosphaera bramlettei

(Hay & Towe, 1962) Bown *et al.*, 2007

Pl. 3, figs 17-18

6.1.7. *Calcidiscus leptoporus* Group

Calcidiscus pataecus Gartner, 1967

Pl. 3, figs 25-40

Remarks: Used herein for small to medium (~3-8 μ m), el-

liptical *Calcidiscus* coccoliths with a closed central area. Specimens were informally divided into less than or greater than 5 μm in length. Larger specimens (>5 μm) appear in Zone NP25. Only consistently present in the site with the best Oligocene preservation (Site U1334; sporadically present at Site U1333), suggesting it is susceptible to dissolution. **Occurrence:** Zone NP23–Zone NN6 (questionable, rare and sporadic occurrences from NP19/20 at Site U1334, but consistently present from NP23); IODP Sites U1332 (one sample), U1333, U1334. Larger specimens (>5 μm) appear in Zone NP25.

Calcidiscus leptoporus (Murray and Blackman, 1898)
Loeblich and Tappan, 1978
Pl. 3, figs 45–48

Remarks: Present from Zone NN2 in Site U1334.

Calcidiscus cf. *C. leptoporus* (Murray and Blackman, 1898) Loeblich and Tappan, 1978
Pl. 3, figs 43–44

Remarks: Small, circular *Calcidiscus* with closed central area.

Calcidiscus premacintyreii Theodoridis, 1984
Pl. 3, figs 49–50

6.1.8. Other calcidiscids

Umbilicosphaera jafari Müller, 1974
Pl. 4, figs 1–4

Remarks: Common from the upper Oligocene (Zone NP24) but present only in the best-preserved samples from Site U1334, suggesting high sensitivity to dissolution. *Umbilicosphaera rotula* is present from Zone NN2.

Umbilicosphaera jordanii Bown, 2005
Pl. 3, figs 21–22

Umbilicosphaera rotula (Kamptner, 1956) Varol, 1982
Pl. 4, figs 5–6

Hayaster perplexus
(Bramlette & Riedel, 1954) Bukry, 1973
Pl. 4, figs 10–11

Family **COCCOLITHACEAE** Poche, 1913 emend.
Young & Bown, 1997

Remarks: The coccolithacean and coccolithacean-like coccoliths are divided here into three informal groups:

1. *Coccolithus pelagicus* Group – *C. pelagicus* and similar coccoliths with narrow central areas that may be spanned by a transverse bar.
2. *Chiasmolithus*–*Cruciplacolithus* Group – forms with central area cross bars.
3. *Clausicoccus* Group – forms with perforate central area plates.

6.1.9. *Coccolithus pelagicus* Group

Coccolithus biparteoperculatus Varol, 1991 comb. nov.
Basionym: *Birkeundia biparteoperculatus*
Varol, 1991, p. 220, pl. 7, figs 11–12. N. Jb. Geol.
Paläont. Abh. 182: 211–237.
Pl. 4, figs 12–18

Remarks: Similar to *Coccolithus pelagicus* but the tube cycle may be indistinct and the narrow central area is filled by a two-part oval bar with a transverse suture. Also similar to *Coccolithus cachaoi* Bown, 2005 but distinguished by the two-part bar. The similarity between these coccolithacean coccoliths has led us to propose this recombination. **Occurrence:** Zone NP15–Zone NP22; IODP Sites U1331–1334. NP12–NP23 (Varol, 1991).

Coccolithus eopelagicus
(Bramlette & Riedel, 1954) Bramlette & Sullivan, 1961
Pl. 4, fig. 27

Coccolithus mutatus (Perch-Nielsen, 1971) Bown, 2005
Pl. 4, fig. 26

Coccolithus pelagicus (Wallich, 1877) Schiller, 1930
Pl. 4, fig. 25

Coccolithus scheri sp. nov.
Pl. 4, figs 19–24

Derivation of name: Named after Howie Scher (University of South Carolina, USA), Exp. 320 shipboard scientist and palaeoceanographer. **Diagnosis:** Small to medium-sized elliptical *Coccolithus* with narrow central area filled by a birefringent broad, oval transverse bar, which is bright at around 45° to the polarizing direction. **Differentiation:** Distinguished from other *Coccolithus* species by the diagnostic birefringent transverse bar. **Remarks:** Most consistently present in the site with best Oligocene preservation (Site U1334), suggesting it is susceptible to dissolution. **Dimensions:** Holotype L = 5.3 μm (Paratype L = 6.0 μm). **Holotype:** Pl. 4, fig. 23. **Paratype:** Pl. 4, fig. 21. **Type locality:** IODP Hole U1334A, Pacific Ocean. **Type level:** Oligocene, Sample U1334A-19H-CC (Zone NP23). **Occurrence:** Zone NP22–Zone NP24; IODP Sites U1332 (one NP23 sample), U1333 (only NP23), U1334.

Ericsonia robusta (Bramlette & Sullivan, 1961)
Edwards & Perch-Nielsen, 1975
Pl. 4, figs 30–32

Remarks: The large variant of this species has a documented last occurrence in the late Paleocene (Raffi *et al.*, 2005) but the smaller form, illustrated here, is occasionally reported above this level. The species is recorded sporadically in the Exp. 320 Eocene sediments, from zones NP12 (Site U1331), NP15 (Site U1333) and NP17–19/20 (Site U1334). This suggests that the species was present throughout the Eocene but was rare and perhaps ecologically restricted.

6.1.10. *Chiasmolithus*–*Cruciplacolithus* Group

Bramletteius serraculoides Gartner, 1969
Pl. 4, figs 33–35

Campylosphaera dela
(Bramlette & Sullivan, 1961) Hay & Mohler, 1967
Pl. 5, fig. 12

Chiasmolithus altus Bukry and Percival, 1971
Pl. 4, figs 39–40

Chiasmolithus gigas
(Bramlette & Sullivan, 1961) Radomski, 1968
Pl. 4, fig. 28

Chiasmolithus grandis
(Bramlette & Riedel, 1954) Radomski, 1968
Pl. 4, fig. 29

Chiasmolithus nitidus Perch-Nielsen, 1971
Pl. 4, fig. 36

Chiasmolithus oamaruensis
(Deflandre, 1954) Hay *et al.*, 1966
Pl. 4, fig. 41

Chiasmolithus titus Gartner, 1970
Pl. 4, figs 37-38

Cruciplacolithus cruciformis
(Hay & Towe, 1962) Roth, 1970
Pl. 5, fig. 11

Cruciplacolithus? klausii sp. nov.
Pl. 5, figs 1-10

Derivation of name: Named after Adam Klaus (IODP, Texas A & M, USA), IODP Expedition 320 shipboard staff scientist and palaeoceanographer. **Diagnosis:** Medium sized (~6-8 μ m), elliptical placolith coccoliths with a low birefringence rim and narrow central area almost filled by broad low birefringence axial cross bars. The brighter tube cycle may be indistinct. **Differentiation:** Distinguished from other *Cruciplacolithus* species by the indistinct tube cycle and low birefringence appearance in XPL. **Remarks:** Only consistently present in the site with best Oligocene preservation (Site U1334), suggesting it is susceptible to dissolution. **Dimensions:** Holotype L = 7.0 μ m (Paratype 6.1 μ m). **Holotype:** Pl.5, fig.1. **Paratype:** Pl.5, fig.3. **Type locality:** IODP Hole U1334A, Pacific Ocean. **Type level:** Upper Oligocene, Sample U1334A-15H-CC (Zone NP25). **Occurrence:** Zone NP21-Zone NP25 (singular occurrence in NP19/20 at U1334); IODP Sites U1332 (one NP23 sample), U1333 (NP22-23), U1334.

Cruciplacolithus cf. *C. primus* Perch-Nielsen, 1977
Pl. 5, figs 13-14

6.1.11. *Clausicoccus* Group

Clausicoccus fenestratus
(Deflandre & Fert, 1954) Prins 1979
Pl. 5, fig. 17

Clausicoccus subdistichus
(Roth & Hay in Hay *et al.*, 1967) Prins, 1979
Pl. 5, figs 15-16

Clausicoccus cf. *C. subdistichus*
(Roth & Hay in Hay *et al.*, 1967) Prins, 1979
Pl. 5, figs 19-20

Remarks: Like *C. subdistichus* but with very narrow central area.

Clausicoccus vanheckiae
(Perch-Nielsen, 1986) de Kaenel & Villa, 1996
Pl. 5, fig. 18

Clausicoccus? sp. rim
Pl. 5, figs 21-23

Remarks: Small bicyclic rims with open central areas but otherwise similar to *C. subdistichus*. Conspicuous in the upper Oligocene/lower Miocene part of Site U1334.

Hughesius gizoensis Varol, 1989
Pl. 5, figs 25-30

Hughesius tasmaniae (Edwards and Perch-Nielsen, 1975) de Kaenel and Villa, 1996
Pl. 5, figs 24, 31-35

Hughesius? sp.
Pl. 5, figs 37-42

Remarks: Small bicyclic coccoliths with very narrow central area but otherwise similar to *Hughesius gizoensis*.

Tetralithoides symeonidesii? Theodoridis, 1984
Pl. 5, figs 36, 43-48

Remarks: Oligocene forms are small inconspicuous coccoliths with four-part plate filling the central area. Reminiscent of the Modern narrow-rimmed placolith group (Young *et al.*, 2003, p. 70) and the Neogene *Tetralithoides symeonidesii* (Pl. 5, fig. 36).

6.1.12. Placolith coccoliths *Incertae Sedis*

Pedinocyclus larvalis Bukry & Bramlette, 1971
Pl. 3, figs 7-9

Pedinocyclus gibbsiae sp. nov.
Pl. 3, figs 10-16

Derivation of name: Named after Samantha Gibbs (University of Southampton, UK) nannopalaeontologist and palaeoceanographer. **Diagnosis:** Medium to large (~6-10 μ m), circular coccoliths with broad rim, narrow, bright inner tube cycle (in XPL) and open central-area. The rim width is just less than half that of the central area (rim width/central area width: ~0.4.) and the rim elements are strongly inclined. **Differentiation:** Distinguished from *Pedinocyclus larvalis* by the relatively narrower rim and wider central area, and from the early Eocene *Geminolithella okayi* Varol, 1989 by the broader inner tube cycle. **Remarks:** Most consistently present in the site with best Oligocene preservation (Site U1334), suggesting it is susceptible to dissolution. **Dimensions:** L = 8.3 μ m (Paratype L = 8.8 μ m). **Holotype:** Pl.3, fig.10. **Paratype:** Pl.3, fig.13. **Type locality:** IODP Hole U1334A, Pacific Ocean. **Type level:** Oligocene, Sample U1334A-19H-CC (Zone NP23). **Occurrence:** Zone NP23-Zone NP25 with rare and sporadic occurrences NP21-22; IODP Sites U1332-1334.

Hayella challengerii (Müller, 1974) Theodoridis, 1984
Pl. 6, figs 1-3

Hayella situliformis Gartner, 1969
Pl. 6, figs 4-5

Iselithina fusa Roth, 1970
Pl. 6, figs 6-9

Ellipsolithus macellus
(Bramlette & Sullivan, 1961) Sullivan, 1964
Pl. 6, figs 10, 11?

6.2. MESOZOIC MUROLITHS

Neocrepidolithus sp. Pl. 6, fig. 12

6.3. CENOZOIC MUROLITHS

Order ZYGODISCALES Young & Bown, 1997

Family **HELICOSPHAERACEAE** Black, 1971

Genus *Helicosphaera* Kamptner, 1954

Remarks: *Helicosphaera* are only present in those Exp. 320 sediments with highest carbonate content, providing strong evidence for the high preservation sensitivity in this group (see also *Pontosphaera*). Occurrences are typically rare and sporadic. We have applied the following informal groups:

1. *Helicosphaera carteri* Group – diffuse birefringent blanket and flange ending with distinct wing (Oligocene-Modern).
2. *Helicosphaera compacta-recta* Group – well-defined and distinctly birefringent blanket (upper Middle Eocene-upper Oligocene: Zone NP17-NN1).
3. *Helicosphaera seminulum* Group – diffuse birefringent blanket, relatively wide central area and disjunct bars (Lower Eocene - Oligocene: Zone NP12-NP25?).

6.3.1. *Helicosphaera carteri* Group

Helicosphaera granulata

(Bukry and Percival, 1971) Jafar and Martini, 1975

Pl. 6, figs 13-18

Helicosphaera intermedia Martini, 1965

Pl. 6, figs 19-24

6.3.2. *Helicosphaera compacta-recta* Group

Helicosphaera clarissima Bown, 2005

Pl. 6, fig. 25

Helicosphaera compacta Bramlette & Wilcoxon, 1967

Pl. 6, figs 26-28

Helicosphaera recta Haq, 1966 (Jafar & Martini, 1975)

Pl. 6, figs 35-39

Helicosphaera reticulata Bramlette & Wilcoxon, 1967

Pl. 6, figs 40-42

Helicosphaera robinsoniae sp. nov.

Pl. 6, figs 29-34

Derivation of name: Named after Rebecca Robinson (University of Rhode Island, USA), Exp. 320 shipboard scientist and palaeoceanographer. **Diagnosis:** Large *Helicosphaera* with birefringent blanket, indistinct but disjunct, birefringent oblique bar, and anterior spur. **Differentiation:** Similar to *H. compacta* and *H. clarissima* but with anterior spur and indistinct disjunct birefringent oblique bar. *H. recta* has a conjunct, transverse bar. **Dimensions:** L = 11.8 µm (Paratype L = 11.6 µm). **Holotype:** Pl. 6, fig. 31. **Paratype:** Pl. 6, fig. 34. **Type locality:** IODP Hole U1334A, Pacific Ocean. **Type level:** Lower Oligocene, Sample U1334A-26X-3, 100 cm (Zone NP21). **Occurrence:** Upper Zone NP21-lower Zone NP22; IODP Sites U1334.

6.3.3. *Helicosphaera seminulum* Group

Helicosphaera bramlettei

(Müller, 1970) Jafar & Martini, 1975

Pl. 6, figs 43-44

Helicosphaera lophota

(Bramlette & Sullivan, 1961) Locker, 1973

Pl. 6, fig. 45

Helicosphaera cf. *H. wilcoxoni* Gartner, 1971

Pl. 6, figs 46-48

Remarks. *Helicosphaera* with open central area spanned by a disjunct transverse bar with dark median suture. The wing morphology is unclear. **Occurrence.** Rare NP21-22, Site U1334.

Family **PONTOSPHAERACEAE** Lemmermann, 1908

Genus *Pontosphaera* Lohmann, 1902

Pl. 7, figs 1-2

Remarks: *Pontosphaera* are very rare and only present in the highest carbonate content sediments of Expedition 320 indicating high preservation sensitivity in this group (see also *Helicosphaera*).

Family **ZYGODISCAEAE** Hay & Mohler, 1967

Isthmolithus recurvus

Deflandre in Deflandre and Fert, 1954

Pl. 7, figs 3-4

Neococcolithes protenus

(Bramlette and Sullivan, 1961) Black, 1967

Pl. 14, figs 1-3

Order SYRACOSPHAERALES Hay, 1977 emend.

Young et al., 2003

Family **SYRACOSPHAERACEAE**

Lemmermann, 1908 *Syracosphaera* sp.

Pl. 7, figs 5-6

Family **RHABDOSPHAERACEAE** Haeckel, 1894

Genus *Blackites* Hay & Towe, 1962

Pl. 7, figs 7-15

Remarks: Can be common from Zone NP15 to NP23 but present only in the better-preserved samples, although typically as disarticulated spines. **Occurrence:** Zone NP15-Zone NP23; IODP Site U1331-1334.

Blackites spines

Pl. 7, figs 8-15

Remarks: The disarticulated spines were identified to species level as follows:

1. *Blackites spinosus* – gently tapering spines with wide axial canal;
2. *Blackites tenuis* – narrow spines with narrow axial canal that initially broaden slightly before gentle tapering;
3. *Pseudotriquetrorhabdulus inversus* – tapers at both ends, ragged appearance and narrow axial canal.

Blackites amplus Roth & Hay, 1967

Pl. 7, fig. 7

Blackites spinosus

(Deflandre & Fert, 1954) Hay & Towe, 1962

Pl. 7, figs 8-9, 13

Blackites tenuis Bramlette and Sullivan, 1961

Pl. 7, figs 14-15

Pseudotriquetrorhabdulus inversus (Bukry & Bramlette, 1969) Wise in Wise & Constans, 1976
Pl. 7, figs 10-12

Remarks: Considered a *Triquetrorhabdulus*-like nannolith by Wise in Wise and Constans (1976) but occurs with other *Blackites* spines here and may represent a distinct species or a preservational (overgrown) morphotype.

6.4. HOLOCOCOLITHS

Family CALYPTROSPHAERACEAE

Boudreaux & Hay, 1967

Zygrhablithus bijugatus bijugatus

(Deflandre in Deflandre & Fert, 1954) Deflandre, 1959

Pl. 13, fig. 46

Remarks: Of the holococcoliths, only one or two specimens of *Z. bijugatus* were found throughout the entire Exp. 320 sample set, illustrating the pervasive effect of dissolution in these deep abyssal-plain sediments. Dissolution susceptible holococcoliths are removed during the long export path from the photic zone or during sedimentation and diagenesis at the sea floor.

6.5. HAPTOPHYTE NANNOLITHS

Family BRAARUDOSPHAERACEAE

Deflandre, 1947

Remarks: No pentoliths (*Braarudosphaera*, *Micrantholithus*, *Pemma*) were observed in the Exp. 320 material, confirming the predominantly neritic distribution of these taxa (e.g., Young *et al.*, 2003).

Family TRIQUETTORHABDULACEAE Lipps, 1969

Genus *Triquetrorhabdulus* Martini, 1965

Pl. 7, figs 16-22

Remarks: These elongate nannoliths are common to abundant in the uppermost Oligocene and lower Miocene, especially in sediments where selective dissolution has concentrated them, together with discoasters. Three species were identified:

1. *T. carinatus* - relatively long with median ridge.
2. *T. longus* - long to very long and narrow.
3. *T. milowii* - short and broad (rice grain shaped); some of these may represent overgrown *T. challengerii* Perch-Nielsen, 1977 specimens, but multiple ridges were not observed.

Triquetrorhabdulus carinatus Martini, 1965

Pl. 7, figs 17-19

Triquetrorhabdulus longus Blaj *et al.*, 2010

Pl. 7, fig. 16

Triquetrorhabdulus milowii Bukry, 1971

Pl. 7, figs 20-22

Orthorhabdus serratus Bramlette and Wilcoxon, 1967

Pl. 7, fig. 23

6.6. EXTINCT NANNOLITHS

Order DISCOASTERALES

Hay, 1977 emend. Bown, 2010

Family DISCOASTERACEAE Tan, 1927

6.6.1. *Discoaster deflandrei* Group

Pl. 7, figs 24-39, Pl. 9, figs 40-41

Remarks: Discoasters with long free-rays that have distinct terminal bifurcations. Species are differentiated based on ray thickness, modal ray number and overall size, e.g. *D. deflandrei* has 5-6 rays, *D. septemradiatus* has 7-8 rays, and *D. nonaradiatus* has 9 rays (but includes 10-12 rays).

Discoaster exilis Martini and Bramlette, 1963

Pl. 7, fig. 37

Discoaster deflandrei Bramlette and Riedel, 1954

Pl. 7, figs 24-27

Discoaster martinii Stradner, 1959

Pl. 7, figs 32-33, 38-39

Discoaster nonaradiatus Klumpp, 1953

Pl. 7, figs 35-36

Discoaster petaliformis Moshkovitz and Ehrlich, 1980

Pl. 9, figs 40-41

Discoaster septemradiatus

(Klumpp, 1953) Martini, 1958

Pl. 7, figs 28-31, 34

6.6.2. *Discoaster nodifer* Group

Pl. 8, figs 1-40

Remarks: Discoasters with short to long free-rays that have paired lateral nodes just before the pointed or notched ray tips. Species herein broadly differentiated on modal ray number and ray length: *D. tanii* has 5 rays, *D. nodifer* has 6-9 rays, *D. druggii* has 6 rays and is large (>15µm), *D. binodosus* has 8 rays with free ray length that approaches half the diameter of the central area or greater, and *D. mediosus* has 10 rays or more with free rays less than half the length of the central area.

Discoaster druggii Bramlette & Wilcoxon, 1967

Pl. 8, fig 18

Discoaster mediosus Bramlette & Sullivan, 1961

Pl. 8, fig. 1-3

Remarks: *Discoaster mediosus* usually has ten rays or more with free rays less than half the length of the central area; *D. binodosus* usually has 8 rays with longer free length and prominent lateral nodes and pointed ray tips (see discussion in Bown, 2005, p. 44). **Occurrence:** Zones NP15-16; IODP Site U1331 (but this site was subject to reworking).

Discoaster nodifer

(Bramlette & Riedel, 1954) Bukry, 1973

Pl. 8, fig. 4-8, 13

Remarks: Six- to nine-rayed stellate discoasters with prominent lateral nodes on their rays and ray-end notches or bifurcations.

Discoaster strictus Stradner, 1961

Pl. 8, fig. 9

Visual identification	Pl., fig. number	base W	base H	base W/H	W/H category	H'	H'/W	H'/base H
<i>S. predistentus</i>	Pl. 11, fig. 15	2.58	0.80	3.23	<i>S. predistentus</i>	4.60	1.78	5.75
<i>S. predistentus</i>	Pl. 11, fig. 17	2.58	0.62	4.16	<i>S. predistentus</i>	4.90	1.90	7.90
<i>S. predistentus</i>	Pl. 11, fig. 19	3.07	0.64	4.80	<i>S. predistentus</i>	4.30	1.40	6.72
<i>S. predistentus</i>	Pl. 11, fig. 20	3.46	0.63	5.49	<i>S. predistentus</i>	7.70	2.23	12.22
<i>S. predistentus</i>	Pl. 11, fig. 21	3.26	0.76	4.29	<i>S. predistentus</i>	7.30	2.24	9.61
<i>S. predistentus</i>	Pl. 11, fig. 23	3.20	1.16	2.76	<i>S. predistentus</i>	8.10	2.53	6.98
<i>S. celsus</i>	Pl. 11, fig. 25	2.93	1.07	2.74	<i>S. predistentus</i>	11.30	3.86	10.56
<i>S. predistentus</i>	Pl. 11, fig. 27	3.91	1.78	2.20	<i>S. distentus</i>	7.60	1.94	4.27
<i>S. akropodus</i>	Pl. 11, fig. 29	3.02	1.33	2.27	<i>S. distentus</i>	7.60	2.52	5.71
<i>S. akropodus</i>	Pl. 11, fig. 31	2.31	1.16	1.99	<i>S. distentus</i>	4.40	1.90	3.79
<i>S. akropodus</i>	Pl. 11, fig. 33	2.58	1.42	1.82	<i>S. distentus</i>	6.60	2.56	4.65
<i>S. akropodus</i>	Pl. 11, fig. 35	2.40	1.25	1.92	<i>S. distentus</i>	6.10	2.54	4.88
<i>S. akropodus</i>	Pl. 11, fig. 37	3.65	1.87	1.95	<i>S. distentus</i>	10.20	2.79	5.45
<i>S. peartiae</i>	Pl. 11, fig. 39	3.29	1.87	1.76	<i>S. distentus</i>	4.10	1.25	2.19
<i>S. peartiae</i>	Pl. 11, fig. 41	3.65	1.87	1.95	<i>S. distentus</i>	6.20	1.70	3.32
<i>S. peartiae</i>	Pl. 11, fig. 43	4.80	2.76	1.74	<i>S. distentus</i>	7.20	1.50	2.61
<i>S. distentus</i>	Pl. 11, fig. 46	3.02	1.42	2.13	<i>S. distentus</i>	5.20	1.72	3.66
<i>S. distentus</i>	Pl. 11, fig. 47	3.29	1.60	2.06	<i>S. distentus</i>	4.00	1.22	2.50
<i>S. distentus</i>	Pl. 12, fig. 1	3.11	1.78	1.75	<i>S. distentus</i>	4.60	1.48	2.58
<i>S. distentus</i>	Pl. 12, fig. 3	3.29	1.78	1.85	<i>S. distentus</i>	5.00	1.52	2.81
<i>S. ciperoensis</i>	Pl. 12, fig. 5	2.94	2.04	1.44	<i>S. ciperoensis</i>	4.00	1.36	1.96
<i>S. ciperoensis</i>	Pl. 12, fig. 7	2.85	1.69	1.69	<i>S. ciperoensis</i>	3.90	1.37	2.31
<i>S. ciperoensis</i>	Pl. 12, fig. 9	2.40	1.69	1.42	<i>S. ciperoensis</i>	3.20	1.33	1.89
<i>S. calyculus</i>	Pl. 12, fig. 11	2.94	2.31	1.27	<i>S. ciperoensis</i>	3.40	1.16	1.47
<i>S. calyculus</i>	Pl. 12, fig. 13	2.49	2.14	1.16	<i>S. ciperoensis</i>	3.50	1.41	1.64
<i>S. calyculus</i>	Pl. 12, fig. 15	2.67	1.87	1.43	<i>S. ciperoensis</i>	4.40	1.65	2.35
<i>S. delphix</i>	Pl. 12, fig. 17	3.56	2.67	1.33	n/a	4.00	1.12	1.50
<i>S. delphix</i>	Pl. 12, fig. 23	3.82	2.67	1.43	n/a	4.40	1.15	1.65
<i>S. delphix</i>	Pl. 12, fig. 25	3.82	2.49	1.53	n/a	4.80	1.26	1.93
<i>S. delphix</i>	Pl. 12, fig. 27	5.16	3.82	1.35	n/a	7.70	1.49	2.02
<i>S. disbelemnus</i>	Pl. 12, fig. 37	2.49	3.56	0.70	n/a	3.90	1.57	1.10
<i>S. disbelemnus</i>	Pl. 12, fig. 39	3.38	4.71	0.72	n/a	5.20	1.54	1.10
<i>S. disbelemnus</i>	Pl. 12, fig. 41	4.09	5.96	0.69	n/a	6.00	1.47	1.01
<i>S. disbelemnus</i>	Pl. 12, fig. 43	2.58	4.18	0.62	n/a	5.10	1.98	1.22
<i>S. belemnus</i>	Pl. 12, fig. 45	3.64	4.44	0.82	n/a	5.60	1.54	1.26
<i>S. heteromorphus</i>	Pl. 12, fig. 47	4.53	3.29	1.38	n/a	7.40	1.63	2.25
<i>S. cf. S. conicus</i> sml.	Pl. 13, fig. 7	3.82	4.45	0.86	n/a	6.10	1.60	1.37
<i>S. conicus</i> s.s.	Pl. 13, fig. 17	7.02	6.85	1.02	n/a	10.20	1.45	1.49
<i>S. cf. S. conicus</i> lge.	Pl. 13, fig. 19	5.87	7.02	0.84	n/a	9.00	1.53	1.28
<i>S. moriformis</i>	Pl. 13, fig. 37	4.27	4.18	1.02	n/a	4.18	0.98	1.00

Table 3. Morphometric data (base height H, base width W, base W/H ratio, H' height to spine bifurcation) for selected illustrated sphenoliths. Base W/H ratio categories are based on Blaj *et al.* (2010): *S. ciperoensis* <1.7, *S. distentus* 1.7-2.5, *S. predistentus* >2.5.

Discoaster tanii Bramlette & Riedel, 1954

Pl. 8, fig. 10-12, 15-17, 19-28

Remarks: Five-rayed stellate discoasters with long free rays terminating in a flat or slightly notched ray-end. Paired lateral nodes are variably developed. Large, three-dimensional specimens (Pl. 8, figs 15-17) and forms with prominent central bosses (Pl. 8, figs 19-28) were distinguished as separate varieties, described below.

Discoaster tanii Bramlette & Riedel, 1954 variety 1

Pl. 8, fig. 15-17

Remarks: Large (typically >15µm), three-dimensional *D. tanii* variety. **Occurrence:** Zone NP17- lower Zone NP24; IODP Site U1334.

Discoaster tanii Bramlette & Riedel, 1954 variety 2

Pl. 8, fig. 19-28

Remarks: Medium to large (9-19µm) *D. tanii* variety with wide central area and prominent boss on one face. The rays are relatively shorter than *D. tanii* s.s. but this

may be due to poor preservation. **Occurrence.** Zones NP18-20; IODP Sites U1331, U1333, U1334.

Discoaster williamsii sp. nov.

Pl. 8, figs 32-40

Derivation of name: Named after Trevor Williams (Lamont Doherty Earth Observatory of Columbia University, USA), IODP Exp. 320 logging staff scientist and palaeoceanographer. **Diagnosis:** Six rayed discoaster with broad central area that is distinctly elevated on both faces. The rays are narrow and free for around half their length. Paired lateral nodes just before the ray tips are present in some specimens (Pl. 8, figs 38-40). **Differentiation:** Distinguished from *D. nodifer* by the broad central area and large central area bosses. **Dimensions:** L = 14.0µm (Paratype L = 13.0µm). **Holotype:** Pl.8, fig.40. **Paratype:** Pl.8, fig.34. **Type locality:** IODP Hole U1331A, Pacific Ocean. **Type level:** Middle Eocene, Sample U1331A-13H-5, 70 cm (Zone NP15). **Occurrence:** Subzone NP15b-Zone NP18/20; IODP Sites U1331-1333.

Discoaster cf. *D. williamsii* sp. nov.

Pl. 8, figs 29-31

Remarks: Like *Discoaster williamsii* but with 5 rays. Similar to some small *D. tani* variety 2 specimens but the central area is elevated on both faces. **Occurrence:** Sub-zone NP15b-Zone NP18/20; IODP Sites U1331-1333.

6.6.3. Rosette discoaster Group

Discoaster barbadiensis Tan, 1927

Pl. 9, figs 13-14

Discoaster bifax Bukry, 1971

Pl. 9, figs 16-23

Discoaster kuepperi Stradner, 1959

Pl. 9, figs 3-5

Discoaster lenticularis Bramlette & Sullivan, 1961

Pl. 9, fig. 6

Discoaster salisburgensis Stradner, 1961

Pl. 9, figs 1-2

Discoaster saipanensis Bramlette and Riedel, 1954

Pl. 9, figs 25-36

Remarks: Morphologically variable in the Exp. 320 material, with 8-5 rays, short to long free rays, but sharing distinctive, sharply tapering ray morphology with pointed ray tips. Six- and five-rayed varieties (distinguished as *D. saipanensis* var. 1 and var. 2) with long free rays and some ray curvature (Pl. 9, figs 30-36) are conspicuous in the upper Eocene (Zones NP17-NP19/20), and reminiscent of the older *D. lodoensis* and *D. sublodoensis* species.

Discoaster saipanensis Bramlette and Riedel, 1954 var. 1

Pl. 9, figs 30-32

Discoaster saipanensis Bramlette and Riedel, 1954 var. 2

Pl. 9, figs 33-36

Discoaster spinescens Bown, 2005

Pl. 9, fig. 15

Discoaster wemmelensis Achuthan and Stradner, 1969

Pl. 9, figs 7-12

6.6.4. Other discoasters

Discoaster lodoensis Bramlette & Riedel, 1954

Pl. 9, figs 37-38

Discoaster sublodoensis Bramlette & Sullivan, 1961

Pl. 9, figs 24, 39

Family **SPHENOLITHACEAE** Deflandre, 1952

Plates 10-13

Remarks: Sphenoliths are common to dominant components of certain Exp. 320 assemblages, especially in the Oligocene to lower Miocene interval. The group is morphologically highly variable and similar morphological features and trends occur repeatedly through their history (Fig. 4). The intergrading morphologies within species plexi result in problematic taxonomy and likely explain inconsistent stratigraphic placement of some datums. This is particularly the case for Oligocene to lower Miocene sphenoliths that have been used in standard nannofossil zonation schemes (*S. ciperoensis*, *S. distentus*) and many taxonomic names are rather poorly constrained (e.g. *S.*

conicus, *S. dissimilis*, *S. calyculus*, etc.). A representative range of morphologies is represented in Plates 10-13 and morphometric data for selected taxa are given in Table 3. A number of informal groups are used, including the *S. radians*, *S. furcatolithoides*, *S. predistentus* and *S. moriformis* groups.

6.6.5. *Sphenolithus radians* Group

Pl. 10, figs 1-49

Remarks: Sphenolith base typically has four distinct quadrants and is square or tapering. In older forms the spines are compound, becoming duo- or monocrystalline in later-appearing forms, and are usually visible but dim at 0° and brightest when at 45° to the polarizing directions; *S. furcatolithoides* spines behave slightly differently. Species are differentiated based on overall height and shape, spine size and degree of taper. *Sphenolithus furcatolithoides*, *S. perpendicularis*, *S. kempii* and *S. cuniculus* form a distinct subgroup with first three/four spines then two separate spines that bifurcate directly above the base. *S. strigosus* has a duocrystalline spine, a higher spine bifurcation point and is dark at 45°. The group contains predominantly Eocene forms, namely: *S. arthuri*, *S. conspicuus*, *S. editus*, *S. orphanknollensis*, *S. pseudoradians*, *S. radians*, *S. spiniger*, *S. villae*; and in the *S. furcatolithoides* subgroup: *S. cuniculus*, *S. furcatolithoides*, *S. perpendicularis*, *S. kempii*, *S. strigosus* and, tentatively, *S. runus*. The species are defined as follows:

1. *Sphenolithus arthuri* Bown, 2005b (not figured here) - like *S. radians* but larger and more coarsely constructed, with blockier spine and base;
2. *Sphenolithus conspicuus* - narrow with a tall spine (dark at 0°, conspicuously bright at 45°) and tall base with long upper quadrants;
3. *Sphenolithus editus* - tapering triangular outline with large and wide lower basal quadrants with sharply tapering spine;
4. *Sphenolithus orphanknollensis* - small, with narrow, tapering spine;
5. *Sphenolithus pseudoradians* - like *S. radians* but larger, more irregular outline and apical cycles that extend laterally beyond the base of the apical spine;
6. *Sphenolithus radians* - square base with equidimensional quadrants and compound tapering spine that may have terminal bifurcations;
7. *Sphenolithus spiniger* - tapering triangular outline with larger lower basal quadrants and a birefringent structure that passes between the basal quadrants at 45° to polarising direction;
8. *Sphenolithus villae* Bown, 2005 (not figured here) - relatively tall base with spine that indents deeply into the upper quadrants;

Sphenolithus furcatolithoides Subgroup

9. *Sphenolithus cuniculus* (not figured here) - like *S. furcatolithoides* but with very short lower quadrants;
10. *Sphenolithus furcatolithoides* - small with two long spines that are bright at 0° (dark at 45°) extending from the upper quadrants;
11. *Sphenolithus perpendicularis* - like *S. furcatolithoides*

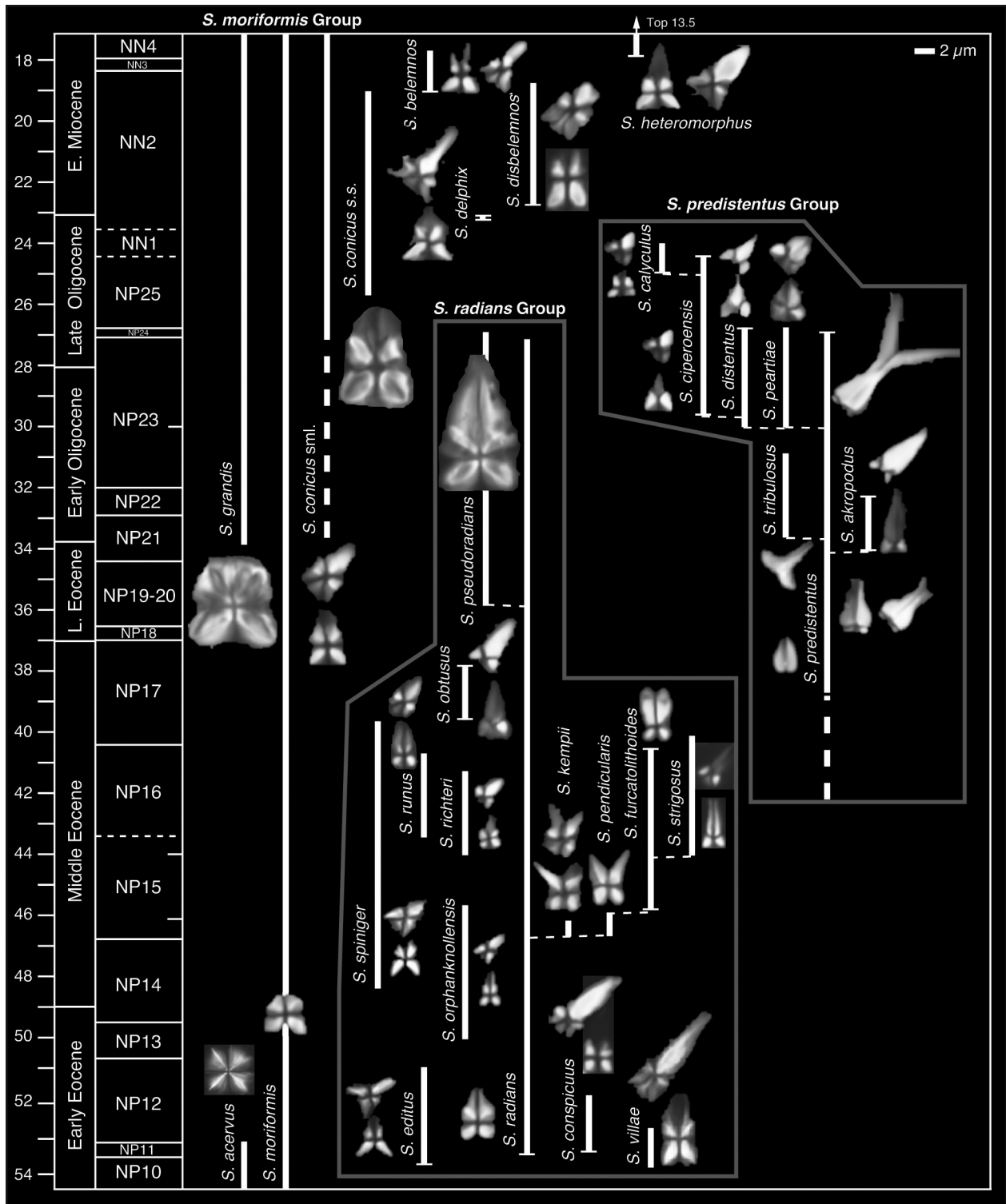


Figure 4. Stratigraphic distribution of Paleogene and early Neogene spenoliths. The timescale is from Pálke *et al.* (2010). Dotted vertical lines are questionable stratigraphic ranges, horizontal bars indicate well constrained range base or top. Informal groups are indicated and phylogenetic inferences are indicated with sloping dotted lines.

- but the two spines are more divergent;
12. *Sphenolithus kempii* – like *S. perpendicularis* but with three or possibly four spines;
 13. *Sphenolithus strigosus* – like *S. furcatolithoides* but the spine bifurcates at a higher level.
 14. *Sphenolithus runus* – narrow with large, lower basal quadrants and spine distinctly bright at 45°.

Other spinose Eocene spenoliths

15. *Sphenolithus richteri* – small and narrow with spine dark at 0° and distinctly bright at 45°.
16. *Sphenolithus obtusus*

Sphenolithus conspicuus Martini 1976
Pl. 10, figs 16-18

*Sphenolithus editus*Perch-Nielsen in Perch-Nielsen *et al.* 1978

Pl. 10, figs 3–4

Sphenolithus orphanknollensis Perch-Nielsen, 1971

Pl. 10, figs 19–24

Sphenolithus pseudoradians Bramlette & Wilcoxon 1967

Pl. 10, figs 1–2

Sphenolithus radians Deflandre in Grassé 1952

Pl. 10, fig. 31

Sphenolithus runus Bown & Dunkley Jones 2006

Pl. 10, figs 48–49

Sphenolithus spiniger Bukry 1971

Pl. 10, figs 5–6

Sphenolithus cf. *S. spiniger*Perch-Nielsen in Perch-Nielsen *et al.* 1978

Pl. 10, figs 7–15

Remarks: Similar to *S. spiniger* but large and coarsely constructed. **Occurrence:** Zones NP17–19/20; IODP Sites U1331–1333.

6.6.6. *Sphenolithus furcatolithoides* Subgroup

Sphenolithus furcatolithoides Locker 1967

Pl. 10, figs 42–43

Sphenolithus perpendicularis Shamrock, 2010

Pl. 10, figs 38–41

Sphenolithus kempii sp. nov.

Pl. 10, figs 25–30, 32–35

Derivation of name: Named after David Kemp (University College London), stratigrapher and palaeoceanographer. **Diagnosis:** Medium sized sphenoliths with three (or possibly four) long spines and square base. At 0° the two outer spines are bright, the middle spine is dark and the base is bright. At 45° the middle spine is bright, the two outer spines are dark and the base is darker and crossed by X-shaped extinction lines. **Remarks:** *S. kempii* has a morphology intermediate between the single spined *S. radians* and the two-spined *S. perpendicularis* and *S. furcatolithoides*, and may be ancestral to these forms. **Differentiation:** Distinguished from most other Eocene sphenoliths by the presence of three discrete spines: otherwise, similar to *S. furcatolithoides*, which has just two outer spines, *S. perpendicularis*, which has two widely divergent outer spines and to *S. radians*, which has just one central spine. **Dimensions:** L = 5.3 µm (Paratypes L = 5.0 µm). **Holotype:** Pl.10, fig.25. **Paratype:** Pl.10, fig.29. **Type locality:** IODP Hole U1333A, Pacific Ocean. **Type level:** Middle Eocene, Sample U1333A-20-2, 50 cm (Zone NP15). **Occurrence:** Lower Zone NP15; IODP Sites U1333.

Sphenolithus cf. *S. kempii* sp. nov.

Pl. 10, figs 36–37

Remarks: Sphenolith seen in top view with four spines arranged as two orthogonal pairs. May represent *S. kempii* specimens, indicating the presence of an additional spine that cannot be seen in more typical side views.

Sphenolithus strigosus Bown & Dunkley Jones 2006

Pl. 10, figs 44–47

6.6.7. Other spinose Eocene sphenoliths

Sphenolithus richteri sp. nov.

Pl. 11, figs 7–12

Derivation of name: Named after Carl Richter (University of Louisiana, USA), Exp. 320 shipboard scientist and palaeomagnetist. **Diagnosis:** Small narrow sphenolith with square base, comprising equidimensional quadrants, and tapering monocrystalline spine that is dark at 0° and bright at 45°. **Differentiation:** Quite distinct from other Eocene sphenoliths, but somewhat similar to Miocene *S. heteromorphus* but the base is square. **Dimensions:** L = 4.3 µm (Paratype L = 3.3 µm). **Holotype:** Pl.11, fig.7. **Paratype:** Pl.11, fig.11. **Type locality:** IODP Hole U1331A, Pacific Ocean. **Type level:** Middle Eocene, Sample U1331A-11H-CC (Zone NP16). **Occurrence:** Zone upper NP15–Zone NP16; IODP Sites U1331 (NP16), U1332 (one upper NP16 sample), U1333.

Sphenolithus obtusus Bukry 1971

Pl. 11, figs 1–6

Occurrence: Zone upper NP16–17; IODP Sites U1331, U1332, U1334.

6.6.8. *Sphenolithus predistentus* Group

Pl. 11, figs 13–48; Pl. 12, figs 1–16

Remarks: A plexus of late Eocene to Oligocene spinose sphenoliths that have been widely used in biostratigraphic zonal schemes (e.g. *S. distentus* and *S. ciperoensis*). The plexus displays great variability, homeomorphic trends and the common occurrence of intergradational forms, which hinders their use as marker species and has been the focus of considerable discussion (e.g., Olafsson and Villa, 1992; Blaj *et al.*, 2010). The morphology is characterised by a base with two, low quadrants (or ‘feet’) that increase in size in younger forms. Spines are tall, duocrystalline, and taper, with terminal bifurcations that may be very long. Older representatives of the group (*S. predistentus*, *S. akropodus*) have duocrystalline spines and low basal ‘feet’ and later forms have relatively larger feet that encroach up the spine, which may appear monocrystalline. The sphenolith basal-width to proximal-cycle-height ratio was considered a useful diagnostic character by Blaj *et al.* (2010), but they did not consider *S. akropodus* or *S. peartiae*, which have ratios identical to *S. distentus*. Nevertheless, generally, *S. predistentus* has basal width/height (W/H) ratios of >2.5, *S. distentus* 1.7–2.5 and *S. ciperoensis* <1.7 (see Table 3). The species herein are defined as follows:

1. *Sphenolithus akropodus* – large with tall, narrow, tapering spine (may appear monocrystalline) and basal ‘feet’ that encroach on the spine; the angle between the top and bottom surface of the feet is up to 90° and the basal W/H ratio is like *S. distentus* (Table 3).
2. *Sphenolithus calyculus* – like *S. ciperoensis* but the base shows four quadrants at 0°.
3. *Sphenolithus celsus* – like *S. predistentus* but with a very tall and narrow spine.
4. *Sphenolithus ciperoensis* – small with relatively large basal ‘feet’ (~half the height of the sphenolith and bas-

al W/H <1.7; Table 3) with low spine that typically appears monocrystalline, and at 45° a birefringent structure passes between the 'feet'.

5. *Sphenolithus distentus* – like *S. akropodus* but smaller with shorter spine that typically appears monocrystalline.
6. *Sphenolithus intercalaris* – small, only the spine is present, most likely due to preservation but probably also reflecting the small size and fragility of the base.
7. *Sphenolithus peartiae* – like *S. predistentus* but when at 45° to the polarising directions a birefringent structure passes between the basal 'feet'.
8. *Sphenolithus predistentus* – small to medium sized, spine with very low base that meets the spine along horizontal or near horizontal sutures.
9. *Sphenolithus tribulosus* – the spine is broadest at the base and tapers sharply, giving an inverted T-shaped outline; the basal 'feet' are small and inconspicuous or absent.

Sphenolithus akropodus de Kaenel & Villa, 1996
Pl. 11, figs 29-38

Remarks: Morphologically similar to *S. distentus* (Table 3), but larger and with a discrete stratigraphic range in the lower Oligocene. **Occurrence:** Zone NP21-Zone NP22; IODP Sites U1332-1334.

Sphenolithus calyculus Bukry, 1985
Pl. 12, figs 11-16

Sphenolithus celsus Haq, 1971
Pl. 11, figs 24-26

Sphenolithus ciperoensis Bramlette and Wilcoxon, 1967
Pl. 12, figs 5-10

Sphenolithus distentus
(Martini, 1965) Bramlette and Wilcoxon, 1967
Pl. 11, figs 45-48; Pl. 12, figs 1-4

Sphenolithus intercalaris Martini, 1976
Pl. 11, fig. 13

Sphenolithus peartiae sp. nov.
Pl. 11, figs 39-44

Derivation of name: Named after Leslie Peart (Consortium for Ocean Leadership, Washington), Exp. 320 ship-board staff educator. **Diagnosis:** Small to medium sized sphenolith with low base that meets the spine along horizontal or near horizontal sutures but when at 45° to polarising direction a birefringent structure passes between the basal 'feet'. **Differentiation:** Like *S. predistentus* but with a basal birefringent structure between the feet, and similar to *S. ciperoensis* but with lower feet that do not insert into the spine and greater base height to width ratio. Similar basal W/H ratio as *S. distentus* (1.74-1.95; Table 3) but has basal birefringent structure. **Dimensions:** Holotype H = 6.20 μm, W = 3.65 μm (Paratype H = 7.20 μm, W = 4.80 μm). **Holotype:** Pl.11, fig.42. **Paratype:** Pl.11, fig.44. **Type locality:** IODP Hole U1334A, Pacific Ocean. **Type level:** Oligocene, Sample U1334A-19H-CC (Zone NP23). **Occurrence:** Zone NP23-Zone NP24; IODP Sites U1331-1334.

Sphenolithus predistentus Bramlette & Wilcoxon 1967
Pl. 11, figs 17-23, 27-28

Remarks: Along with *S. moriformis*, this is the most common and consistently occurring sphenolith through the Oligocene section. It is highly variable in size and intergrades with *S. akropodus*, *S. distentus* and *S. peartiae*.

Sphenolithus tribulosus Roth, 1970
Pl. 11, fig. 14

6.6.9. Other sphenoliths

Sphenolithus belemnus Bramlette and Wilcoxon, 1967
Pl. 12, figs 45-46

Sphenolithus delphix Bukry, 1973
Pl. 12, figs 23-28

Sphenolithus cf. *S. delphix* Bukry, 1973
Pl. 12, figs 17-22

Remarks: Like *S. delphix* but more coarsely constructed and with a relatively lower, broader spine.

Sphenolithus disbelemnus Fornaciari and Rio, 1996
Pl. 12, figs 37-44

Sphenolithus heteromorphus Deflandre, 1953
Pl. 12, figs 47-48

Sphenolithus procerus? Maiorano & Monechi, 1997
Pl. 12, figs 29-36

Remarks: Low basal quadrants are wider than the upper quadrants and the spine is duocrystalline, gently tapering and brightest at 45°. First described from Zone NN2 but occurs slightly earlier here (Zones NP25 and NN1). **Occurrence:** Zones NP25-NN2, Sites U1333-1334; Zone NN2, DSDP Site 563, N. Atlantic (Maiorano and Monechi, 1997)

6.6.10. *Sphenolithus moriformis* Group

Sphenolithus conicus Bukry 1971 *sensu stricto*
Pl. 13, figs 13-18

Remarks: Described by Bukry (1971) as a 'large', 'tall' 'triangular' species (7-12 μm) but applied more broadly in the literature to include smaller, triangular forms. The name is applied here to large forms only (>7 μm in height), which are particularly conspicuous in the Oligocene/Miocene boundary interval. These sphenoliths are coarsely constructed with a high, gently tapering base and a short tapering spine. The base is typically longer than the spine, with the lower quadrants slightly larger than the upper. The spine is composite, dark at 0° and bright at 45°. In XPL the sphenolith shows high birefringence colours of yellow, orange and blue. Similar sphenoliths that are smaller were differentiated as *Sphenolithus* cf. *S. conicus* 'small variety' in this study. **Occurrence:** Zone NP25-NN2; IODP Sites U1333, U1334.

Sphenolithus cf. *S. conicus* Bukry 1971 small variety
Pl. 13, figs 1-12

Remarks: Medium sized sphenoliths with a gently tapering base and short tapering spine. The base has four quadrants and is typically taller than or similar in length to the spine, with the lower quadrants slightly larger than the upper. Specimens with slightly taller spines were informally differentiated. The spine is composite, dark at 0°

and bright at 45°. **Differentiation:** A somewhat generalized spenolith morphology but the spine is taller than *S. moriformis* and it is smaller than *S. conicus* s.s. May intergrade with *Sphenolithus abies* Deflandre in Deflandre & Fert, 1954. Occurrence: Zone NP22-NN15; IODP Sites U1331-U1334.

Sphenolithus cf. *S. conicus* Bukry 1971 large variety
Pl. 13, figs 19-28

Remarks: A large (~7 µm), coarsely constructed spenolith with a high, parallel-sided base and a short spine. Similar to *S. conicus* s.s. but the base is typically longer than the spine, with the lower quadrants larger than the upper. The spine is composite, dark at 0° and bright at 45°. In XPL the spenolith shows high birefringence colours of yellow, orange and blue. **Occurrence:** Zone NN2; IODP Sites U1334.

Sphenolithus sp. 1
Pl. 13, figs 29-36

Remarks: Large, coarsely constructed spenolith with lower basal quadrants that are larger than the upper quadrants and the spine is duocrystalline with near parallel sides and a blunt termination. Similar in general morphology to *S. procerus*. **Occurrence:** Not well constrained, but Zones NP21-23 and possibly younger occurrences up to NN2; Sites U1332-1334.

Sphenolithus moriformis (Brönnimann & Stradner, 1960)
Bramlette & Wilcoxon, 1967
Pl. 13, fig. 37

Sphenolithus grandis Haq and Berggren, 1978
Pl. 13, fig. 38-41

Remarks: Used here for large (>7 µm) *S. moriformis*-like spenoliths.

6.6.11. Incertae Sedis Nannoliths

Lapideacassis Black 1971 sp.
Pl. 13, fig. 45

Remarks: Very rare (middle Eocene, Site U1331).

Nannotetrina Achuthan and Stradner, 1969
Pl. 14, figs 6-46

Remarks: These cruciform nannoliths form conspicuous components of the Exp. 320 middle Eocene sections and are divided herein as follows:

1. *Nannotetrina* sp. 1 – small, with broadly square outline;
2. *Nannotetrina* cf. *N. alata* – small, short arms with blunt terminations;
3. *Nannotetrina alata* – long arms with blunt terminations;
4. *Nannotetrina fulgens* – long tapering arms with pointed terminations;
5. *Nannotetrina cristata* – three dimensional with curving arms and inter-arm fill;
6. *Nannotetrina spinosa* – broadly square with elongations from the corners and shorter spines from the sides resulting in an stellate (eight-pointed) symmetrical outline;

cal outline;

7. *Nannotetrina pappii* – broadly square to cruciform with spinose projections resulting in a stellate (eight-pointed) asymmetrical outline.

Other nannofossils with similar appearance include four-rayed discoasters, e.g. *Discoaster cruciformis* (Plate 14, figs 4-5) and disarticulated cross-bars of *Neococcolithes protenus* (see Plate 14, figs 1-3).

Nannotetrina sp. 1

Pl. 14, figs 6-8

Nannotetrina cf. *N. alata*

(Martini, 1960) Haq and Lohmann, 1976

Pl. 14, figs 9-12

Nannotetrina alata

(Martini, 1960) Haq and Lohmann, 1976

Pl. 14, figs 13-18

Nannotetrina cristata

(Martini, 1958) Perch-Nielsen, 1971

Pl. 14, figs 19-24

Nannotetrina fulgens (Stradner in Martini & Stradner, 1960) Achuthan & Stradner, 1969

Pl. 14, figs 25-29

Nannotetrina spinosa

(Stradner in Martini & Stradner, 1960) Bukry, 1973

Pl. 14, figs 31-42

Nannotetrina pappii

(Stradner, 1959) Perch-Nielsen, 1971

Pl. 14, figs 30, 43-46

Tribrachiatus orthostylus Shamrai, 1963

Pl. 14, fig. 47

L-shaped liths Pl. 13, fig. 37-38

Remarks: L-shaped liths of uncertain affinity are occasionally common.

Acknowledgements

Thanks to IODP Expedition 320 operational and technical staff and shipboard science party for facilitating such an enjoyable and successful drilling expedition. This research used samples and/or data provided by the Integrated Ocean Drilling Program (IODP). Funding for this research was provided by the Natural Environment Research Council. We very much appreciate the careful and constructive reviews of Jean Self-Trail, Liam Gallagher and other reviewers.

References

- Agnini, C., Muttoni, G., Kent, D.V. & Rio, D. 2006. Eocene biostratigraphy and magnetic stratigraphy from Possagno, Italy: The calcareous nannofossil response to climate variability. *Earth and Planetary Science Letters*, **241**: 815-830.
- Blaj, T., Henderiks, J., Young, J.R. & Rehnberg, E. 2010. The Oligocene nannolith *Sphenolithus* evolutionary lineage: morphometrical insights from the palaeo-equatorial Pacific Ocean. *J. of Micropalaeontology*, **29**: 17-35.
- Blaj, T. & Young, J.R. 2010. A new Oligocene *Tri-*

- quetrorhabdulus* species, *T. longus* sp. nov. *Journal of Nannoplankton Research*, **31**: 1-4.
- Bown, P.R., 2005. Palaeogene calcareous nannofossils from the Kilwa and Lindi areas of coastal Tanzania (Tanzania Drilling Project 2003-4). *Journal of Nannoplankton Research*, **27**: 21-95.
- Bown, P.R. 2005b. Calcareous nannofossil biostratigraphy of the Cenozoic of Leg 198 Site 1208, Shatsky Rise, northwest Pacific Ocean.). In: Bralower, T.J., Premoli Silva, I., and Malone, M.J. (Eds.), *Proceedings of the Ocean Drilling Program, Scientific Results*, **198**: 1-44. [Online]. http://www-odp.tamu.edu/publications/198_SR/104/104.htm.
- Bown, P.R., Dunkley Jones, T. & Young, J.R. 2007. *Umbilicosphaera jordanii* Bown, 2005 from the Paleogene of Tanzania: confirmation of generic assignment and a Paleocene origination for the family Calcidiscaceae. *Journal of Nannoplankton Research*, **29**: 25-30.
- Bown, P.R. & Young, J.R. 1998. Techniques. In: Bown, P.R. (Ed.). *Calcareous Nannofossil Biostratigraphy*. Kluwer Academic, London: 16-28.
- Bown, P.R. & Dunkley Jones, T. 2006. New Paleogene calcareous nannofossil taxa from coastal Tanzania: Tanzania Drilling Project Sites 11 to 14. *Journal of Nannoplankton Research*, **28**: 17-34.
- Bralower, T.J. & Mutterlose, J. 1995. Calcareous nannofossil biostratigraphy of Site 865, Allison Guyot, Central Pacific Ocean: a tropical Paleogene reference section. *Proceedings of the ODP, Scientific Results*, **143**: 31-74.
- Bukry, D. 1971. Cenozoic calcareous nannofossils from the Pacific Ocean. *San Diego Society of Natural History, Transactions*, **16**: 303-327.
- Dunkley Jones, T., Bown, P.R. & Pearson, P.N. 2009. Exceptionally well preserved upper Eocene to lower Oligocene calcareous nannofossils from the Pande Formation (Kilwa Group), Tanzania. *J. Systematic Palaeontology*, **7**: 359-411.
- Firth, J. 1992. Analysis of the taxonomic, biostratigraphic and evolutionary relationships of species of the calcareous nannofossil genus *Cyclicargolithus* (Bukry, 1971) from the upper Eocene and Oligocene of the North Atlantic. *Memorie di Scienze Geologiche*, **43**, 237-259.
- Fornaciari, E., Agnini, C., Catanzariti, R., Rio, D., Bolla, E.M. & Valvasoni, E. 2010. Mid-Latitude calcareous nannofossil biostratigraphy and biochronology across the middle to late Eocene transition. *Stratigraphy*, **7**: 229-264.
- Gallagher, L.T. 1989. *Reticulofenestra*: A critical review of taxonomy, structure and evolution. In: J.A. Crux and S.E. van Heck (eds). *Nannofossils and their applications*, Ellis Horwood, Chichester: 41-75.
- de Kaenel, E. & Villa, G. 1996. Oligocene-Miocene calcareous nannofossil biostratigraphy and paleoecology from the Iberia Abyssal Plain. *Proceedings of the ODP, Scientific Results*, **149**: 79-145.
- Jordan, R.W., Kleijne, A. & Young, J.R. 2004. A revised classification scheme for living haptophytes. *Micropaleontology*, **50**: 55-79.
- Maiorano, P. 2006. *Reticulofenestra circus* var. *lata* n. var.: a large reticulofenestrid (Coccolithophoridae) from the Early Oligocene. *Micropaleontology*, **52**: 81-86.
- Maiorano, P. & Monechi, S. 1997. Revised correlations of Early and Middle Miocene calcareous nannofossil events and magnetostratigraphy from DSDP Site 563 (North Atlantic Ocean). *Marine Micropaleontology*, **35**: 235-255.
- Martini, E. 1971. Standard Tertiary and Quaternary calcareous nannoplankton zonation. In: A. Faranacci (Ed.) *Proceedings of the Second Planktonic Conference Roma 1970*. Edizioni Tecnoscienza, Rome, **2**: 739-785.
- Olafsson, G. 1992. Oligocene/Miocene morphometric variability of the *Cyclicargolithus* group from the equatorial Atlantic and Indian Oceans. *Memorie di Scienze Geologiche*, **43**: 283-296.
- Olafsson, G. & Villa, G. 1992. Reliability of sphenoliths as zonal markers in Oligocene sediments from Atlantic and Indian Oceans. *Memorie di Scienze Geologiche*, **43**: 261-275.
- Pälike, H., Nishi, H., Lyle, M., Raffi, I., Gamage, K., Klaus, A., and the Expedition 320/321 Scientists. 2010. Pacific Equatorial Transect. *Proceedings of the Integrated Ocean Drilling Program*, **320/321**: Tokyo (Integrated Ocean Drilling Program Management International, Inc.). doi:10.2204/iodp.proc.320321.2010 [online: http://publications.iodp.org/proceedings/320_321/32021title.htm]
- Pälike, H. et al. submitted. A new Cenozoic record of Equatorial Pacific carbonate accumulation rates and compensation depth.
- Perch-Nielsen, K., 1985. Cenozoic calcareous nannofossils. In: H.M. Bolli, J.B. Saunders & K. Perch-Nielsen (Eds.). *Plankton Stratigraphy*. Cambridge University Press, Cambridge: 427-554.
- Raffi, I., Backman, J. & Pälike, H. 2005. Changes in calcareous nannofossil assemblages across the Paleocene/Eocene transition from the Paleo-equatorial Pacific Ocean. *Palaeogeography, Palaeoclimatology, Palaeoecology*, **226**: 93-126.
- Shamrock, J. 2010. A new calcareous nannofossil species of the genus *Sphenolithus* from the Middle Eocene (Lutetian) and its biostratigraphic significance. *Journal of Nannoplankton Research*, **31**: 5-10.
- Varol, O. 1989. Eocene calcareous nannofossils from Sile (northwest Turkey). *Revista Espanola de Micropaleontologia*, **21**: 273-320.
- Varol, O. 1991. New Cretaceous and Tertiary Calcareous Nannofossils. *Neues Jahrbuch für Geologie und Paläontologie, Abhandlungen*, **182**: 211-237.
- Westerhold, T. and the Expedition 320/321 Scientists. 2011. Revised composite depth scales and integration of IODP Sites U1331-U1334 and ODP Sites 1218-12201. *Proceedings of the Integrated Ocean Drilling Program*, **320/321**: Tokyo (Integrated Ocean Drilling Program Management International, Inc.). doi:10.2204/iodp.proc.320321.201.2011 [online:

- tions.iodp.org/proceedings/320_321/32021toc.htm]
- Wise, S.W. & Constans, R.E. 1976. Mid Eocene plankton correlations Northern Italy-Jamaica, W.I. . *Gulf Coast Assoc. Geol. Soc., Trans.*, **26**:144-155.
- Young, J.R. 1990. Size variation of Neogene *Reticulofenestra* coccoliths from the Indian Ocean DSDP cores. *J. Micropalaeontology*, **9**: 71-85.
- Young, J.R. 1998. Neogene. In: P.R. Bown (Ed.). *Calcareous Nannofossil Biostratigraphy*. Kluwer Academic, London: 225-265.
- Young, J.R. & Bown, P.R. 1997. Cenozoic calcareous nannoplankton classification. *Journal of Nannoplankton Research*, **19**: 36-47.
- Young, J.R., Bergen, J.A., Bown, P.R., Burnett, J.A., Fiorentino, A., Jordan, R.W., Kleijne, A., van Niel, B.E., Romein, A.J.T. & von Salis, K. 1997. Guidelines for coccolith and calcareous nannofossil terminology. *Palaeontology*, **40**: 875-912.
- Young, J.R., Geisen, M., Cros, L., Kleijne, A., Sprengel, C., Probert, I. & Ostergaard, J. 2003. A guide to extant coccolithophore taxonomy. *Journal of Nannoplankton Research Special Issue* **1**.

Plate 1

Reticulofenestra umbilicus Group, Reticulofenestra lockeri Group, Reticulofenestra reticulata Group

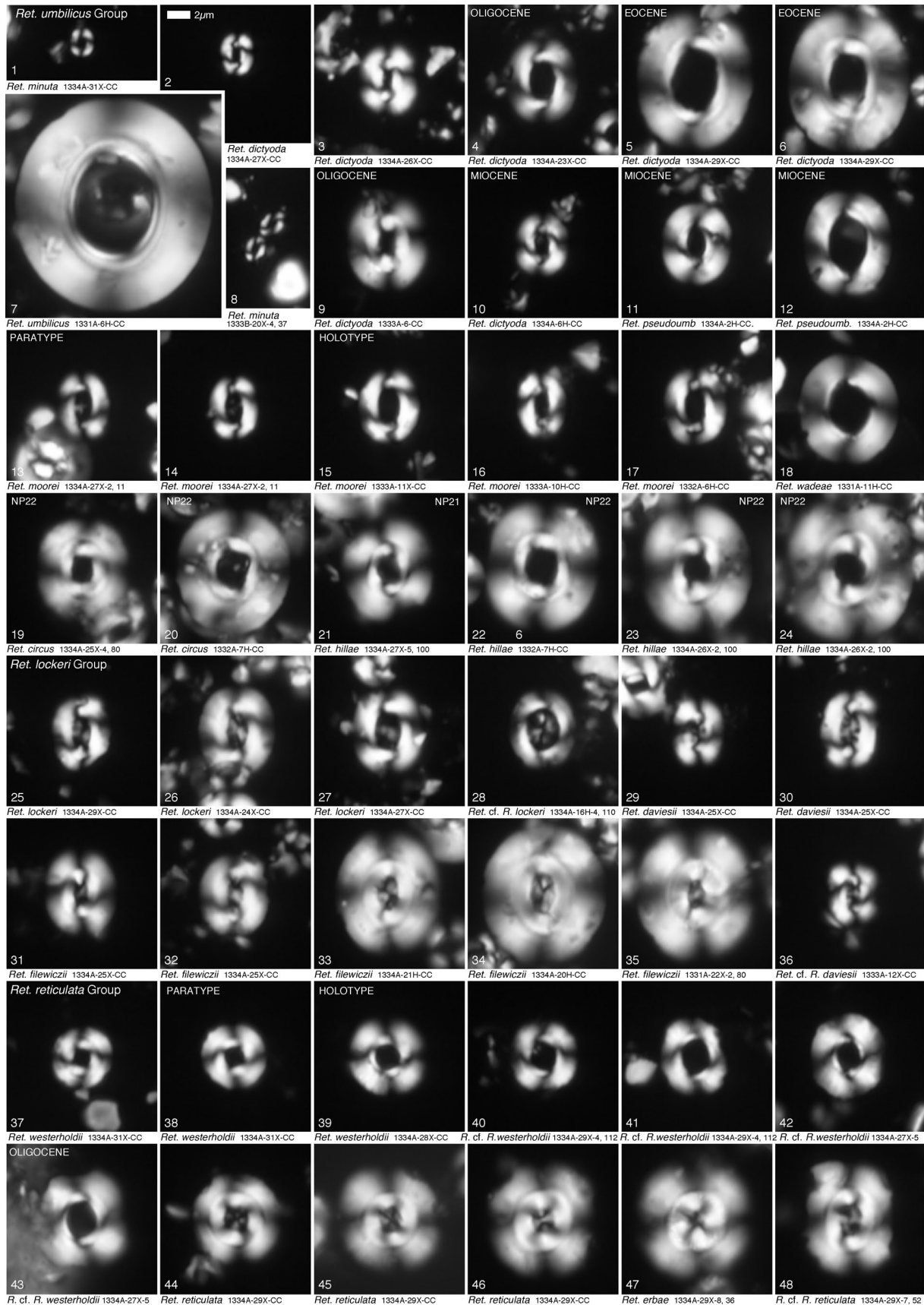


Plate 2

Reticulofenestra reticulata Group, Cyclicargolithus floridanus Group, Reticulofenestra bisecta Group, Prinsiaceae,
Paleogene calcidiscid Group

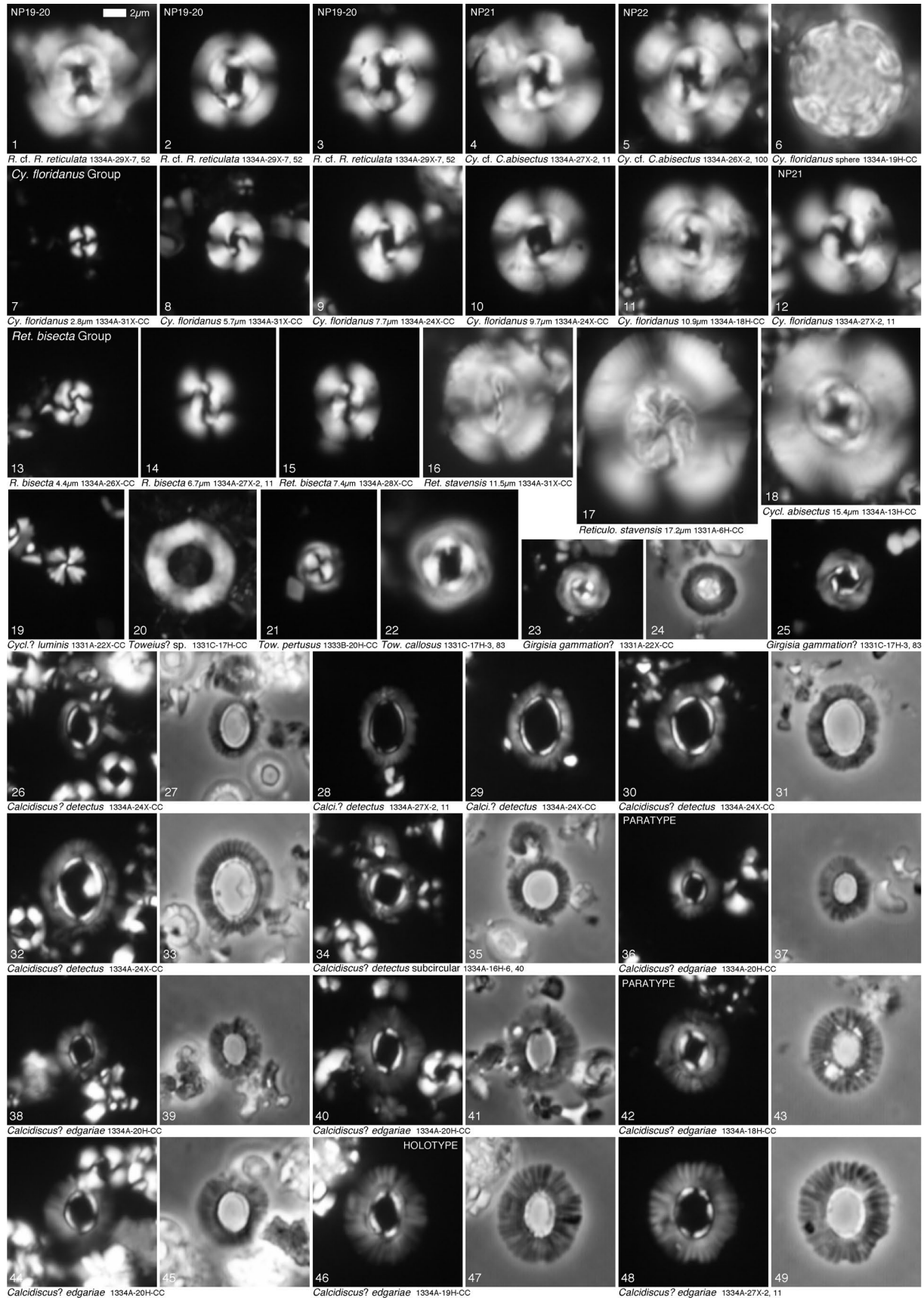


Plate 3

Paleogene calcidiscid Group, Placolith coccoliths incertae sedis, Calcidiscus leptoporus Group

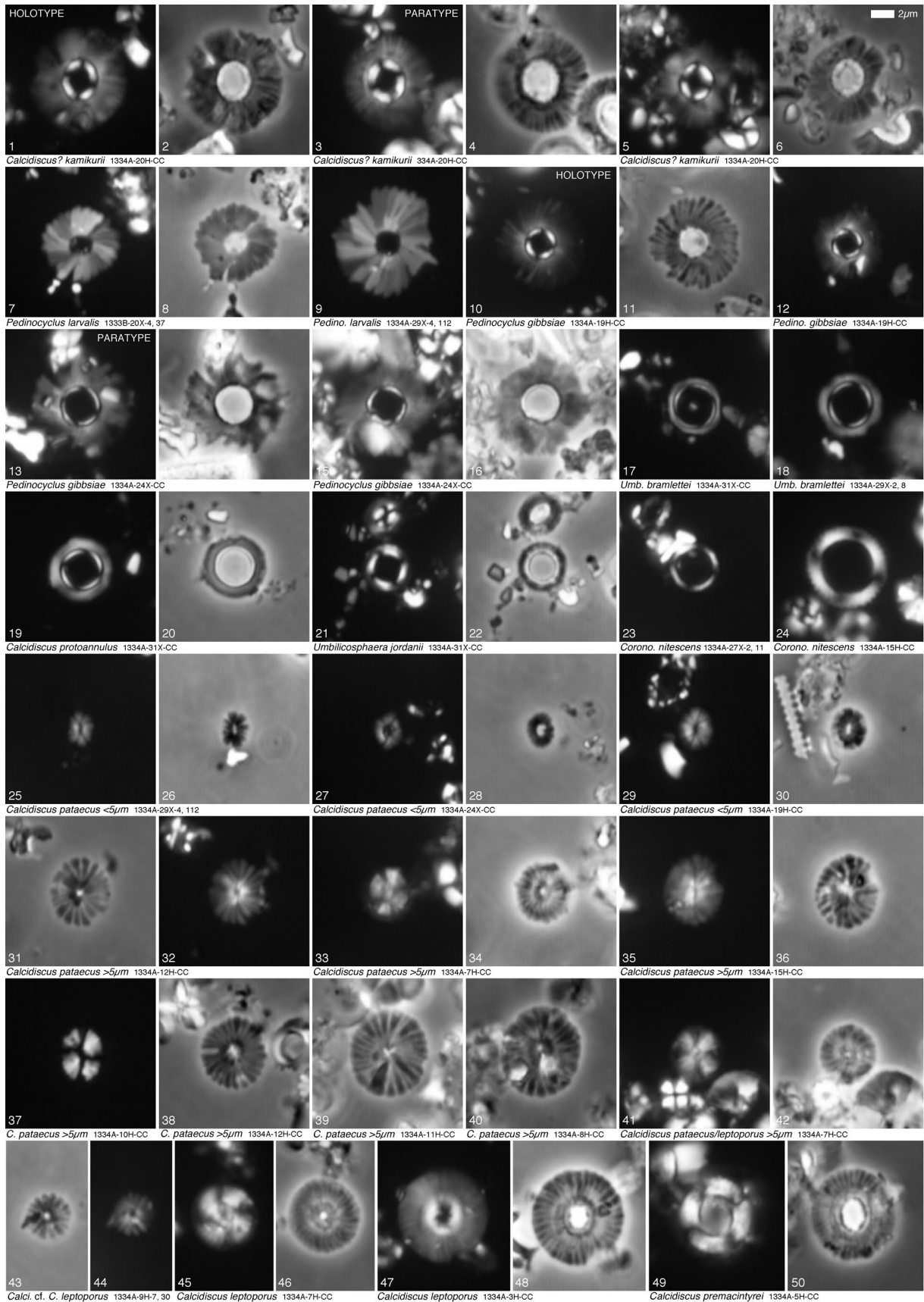


Plate 4

Other calcidiscids, Paleogene calcidiscid Group, Coccolithus pelagicus Group, Chiasmolithus
- Crucioplacolithus Group

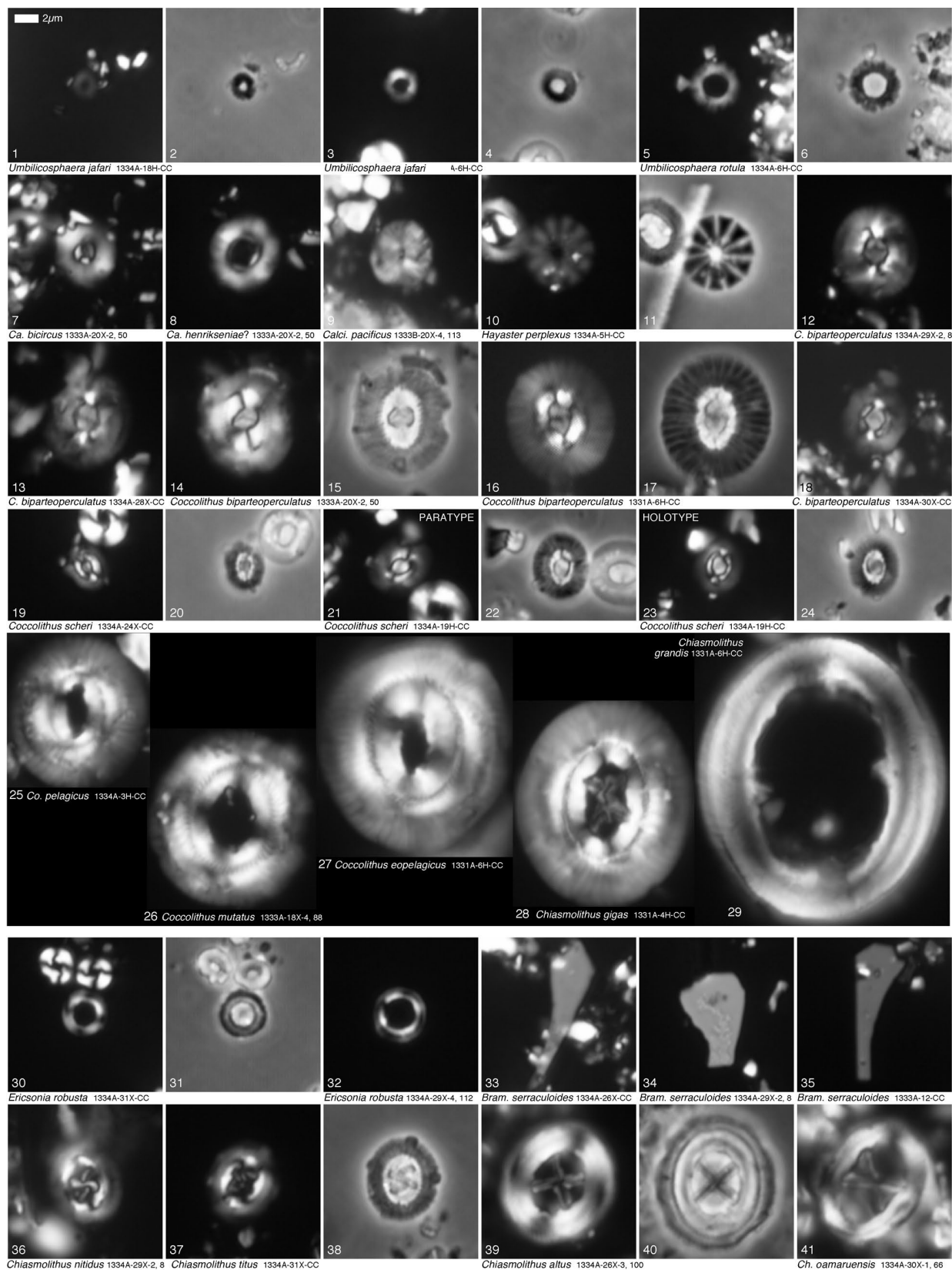


Plate 5

Chiasmolithus - Cruciplacolithus Group, Clausicoccus Group

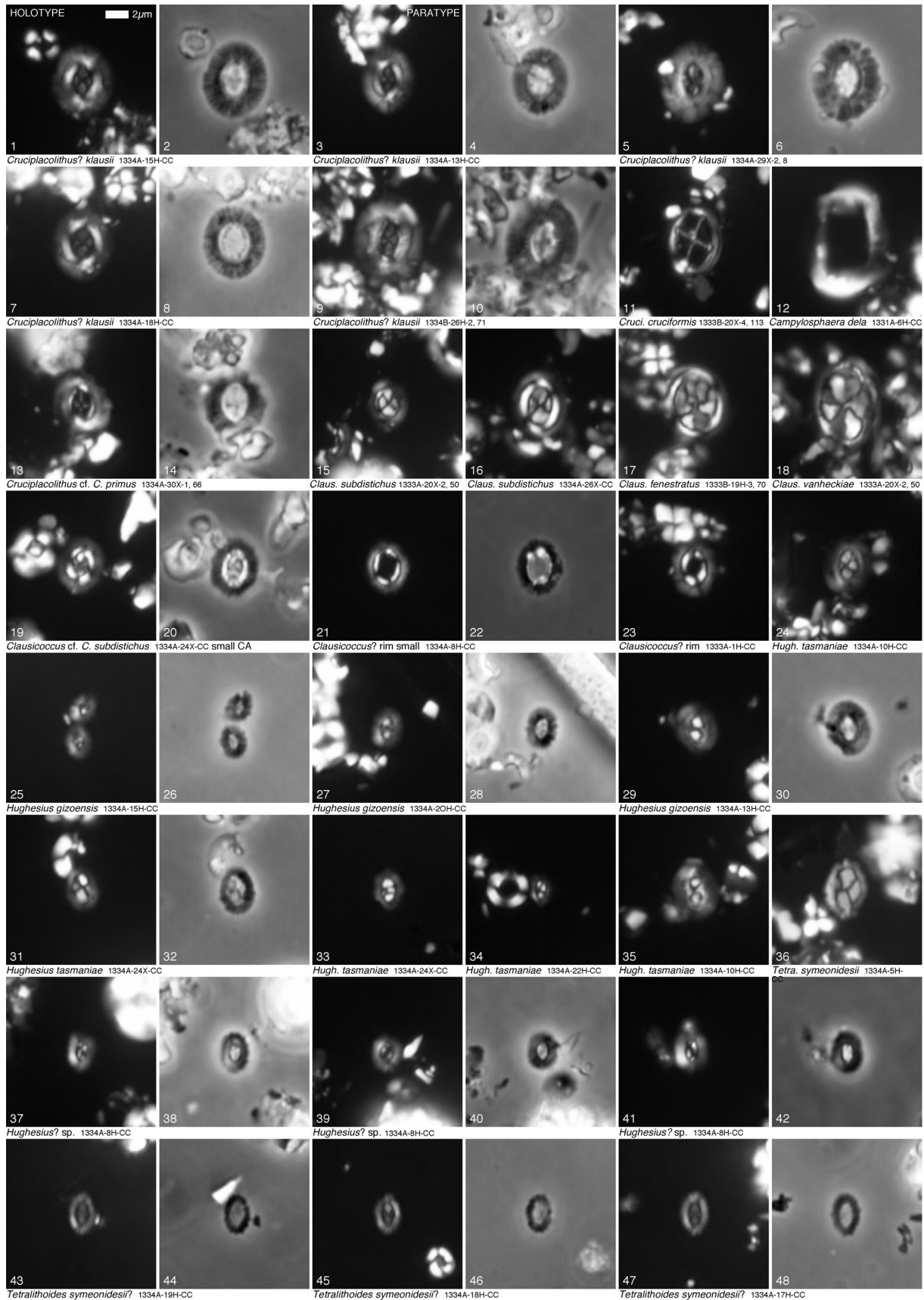


Plate 6

Placolith coccoliths incertae sedis, Mesozoic muroliths, *Helicosphaera carteri* Group,
Helicosphaera compacta-recta Group, *Helicosphaera seminulum* Group

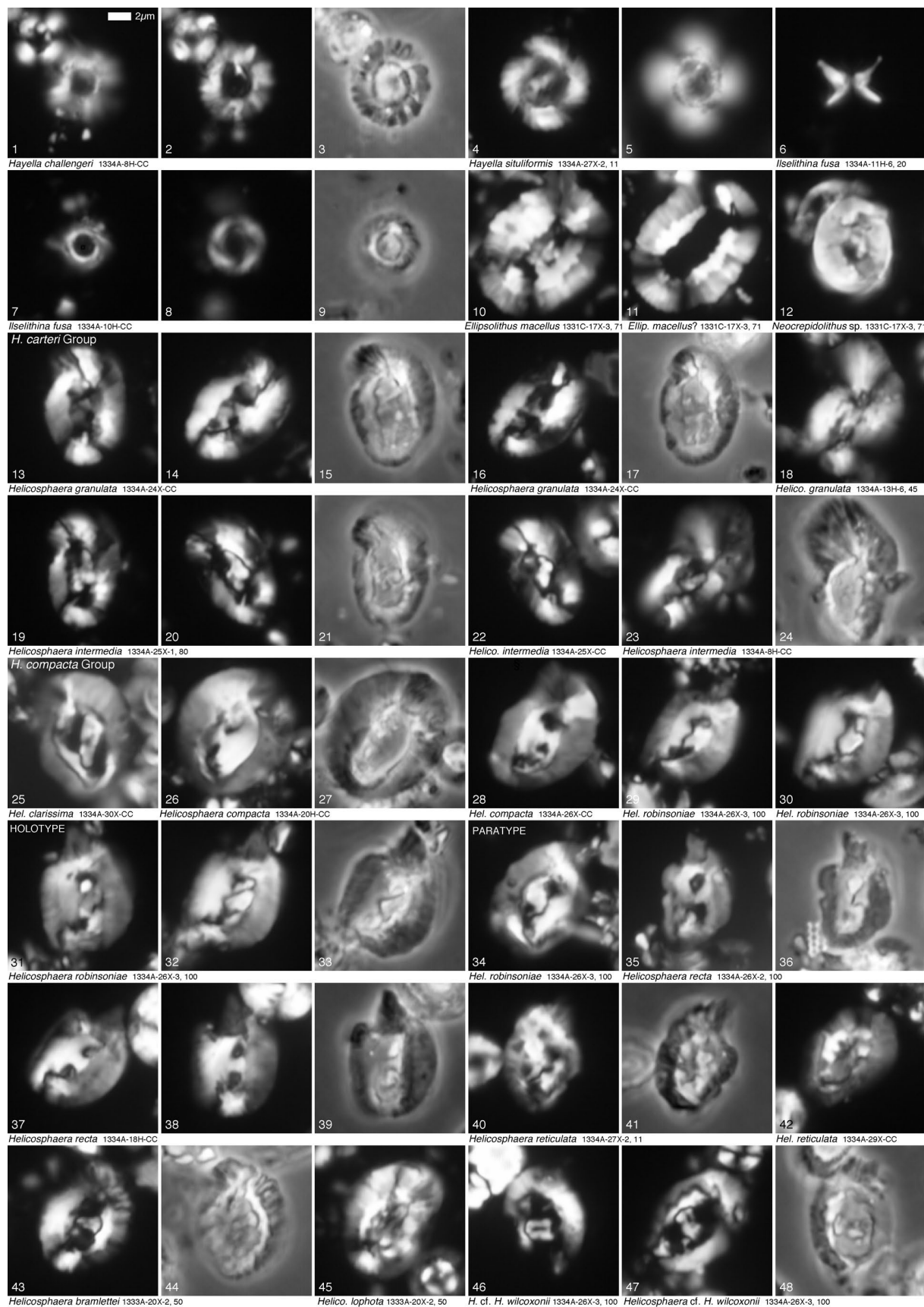


Plate 7

Pontosphaeraceae, Rhabdosphaeraceae, Triquetrorhabdulaceae, Discoaster deflandrei Group

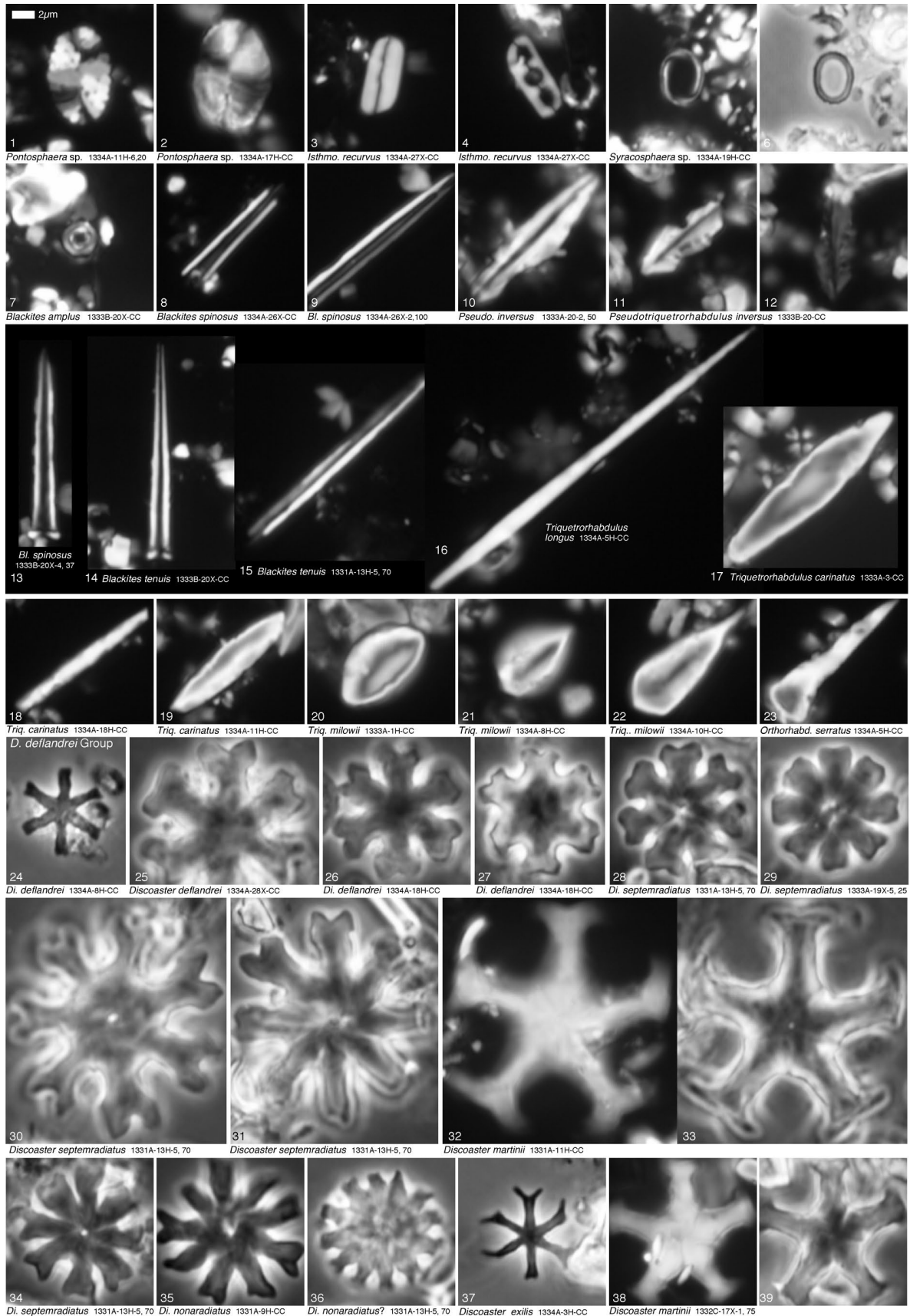


Plate 8

Discoaster nodifer Group

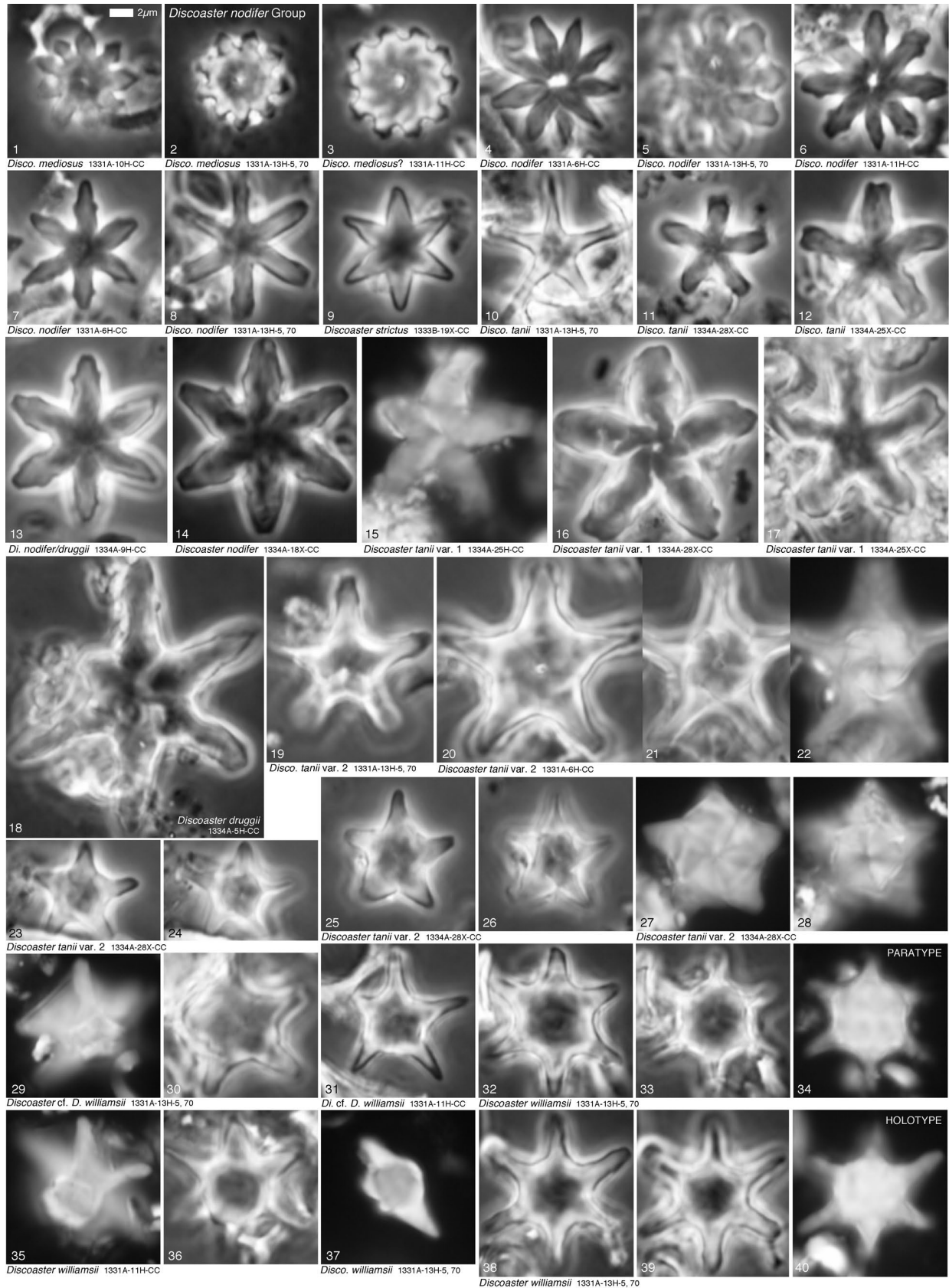


Plate 9

Rosette discoaster Group, Other discoasters

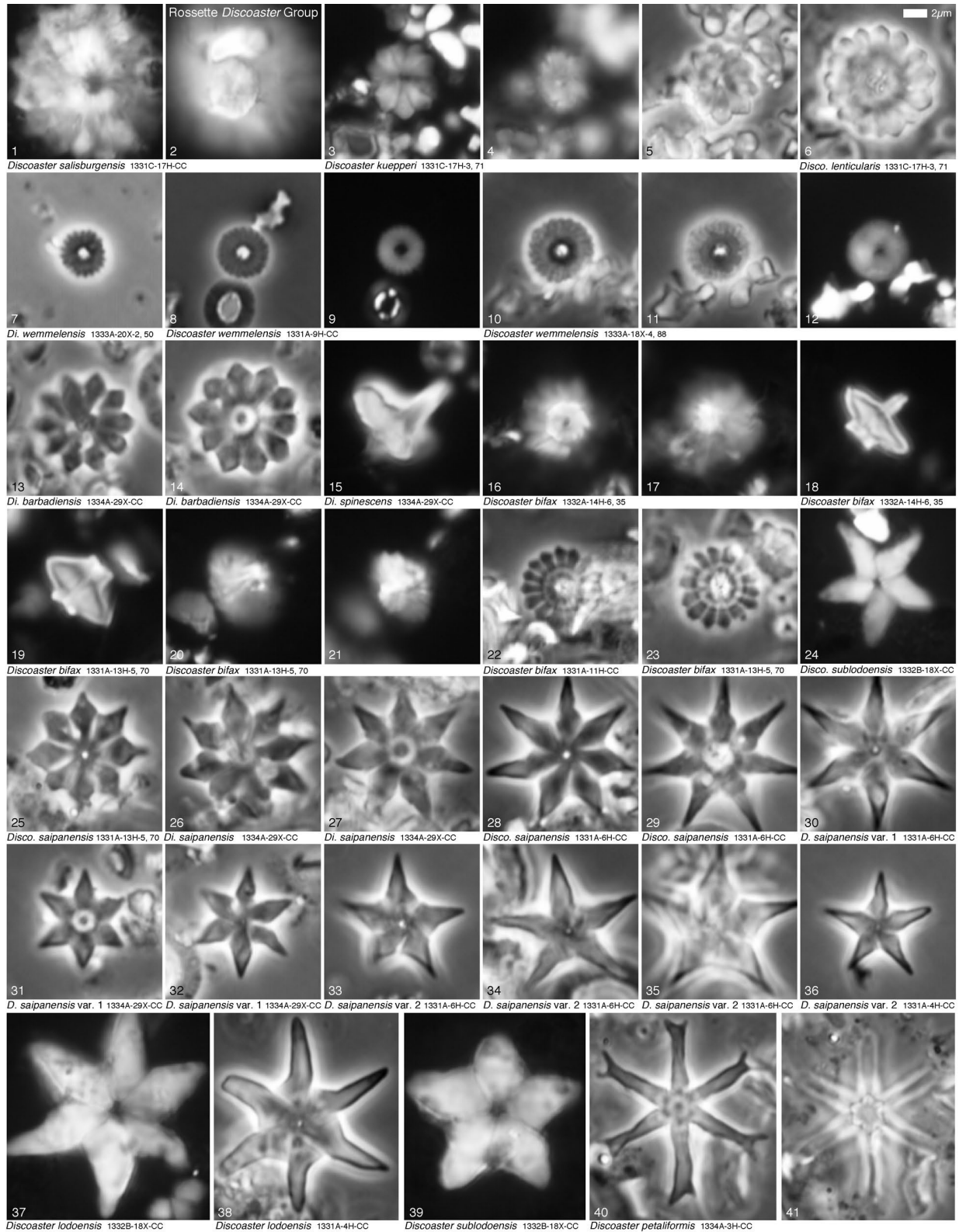


Plate 10

Sphenolithus radians Group

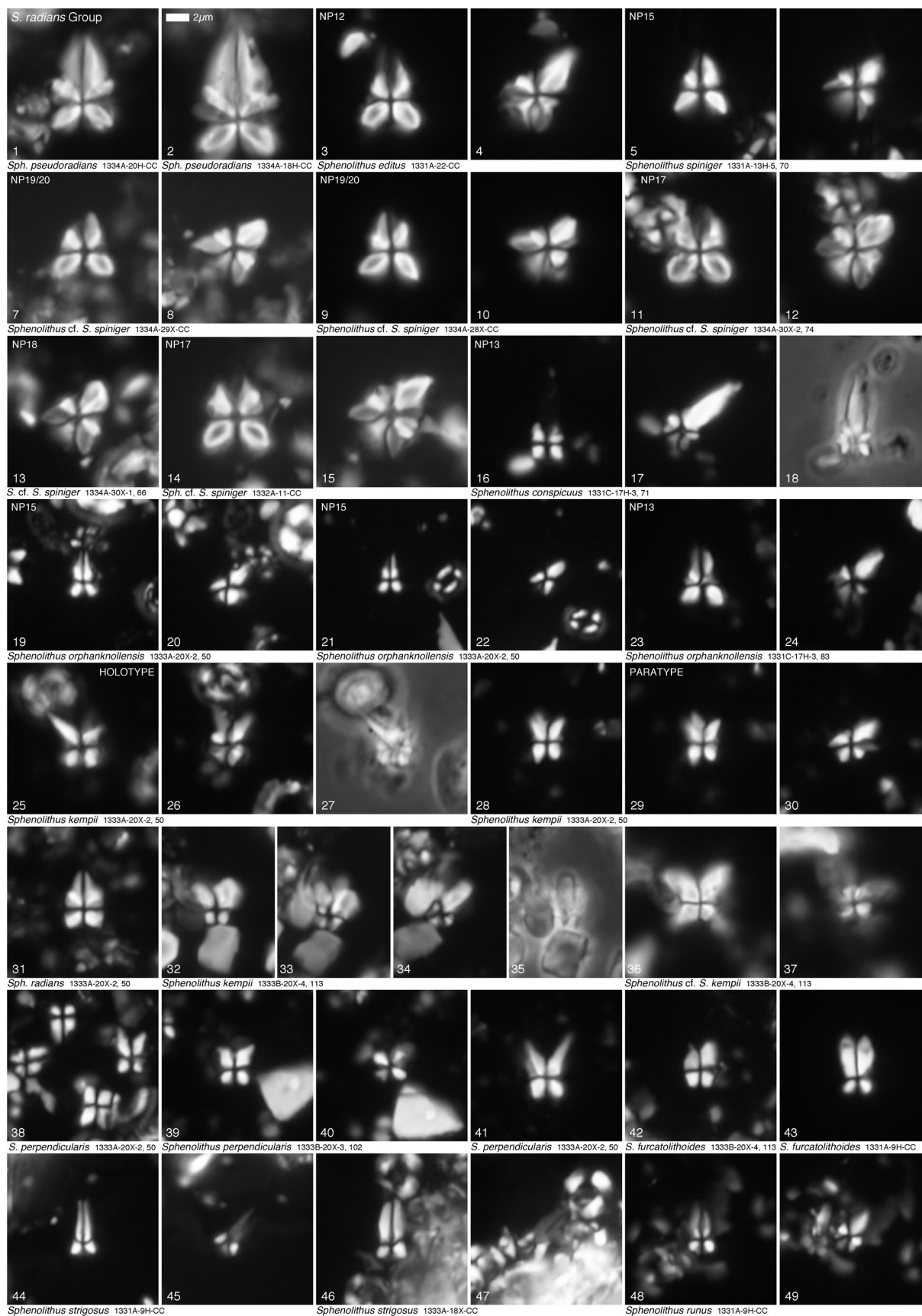


Plate 11

Sphenolithus radians Group, other spinose Eocene sphenoliths, Sphenolithus predistentus Group



Plate 12

Sphenolithus predistentus Group, other sphenoliths

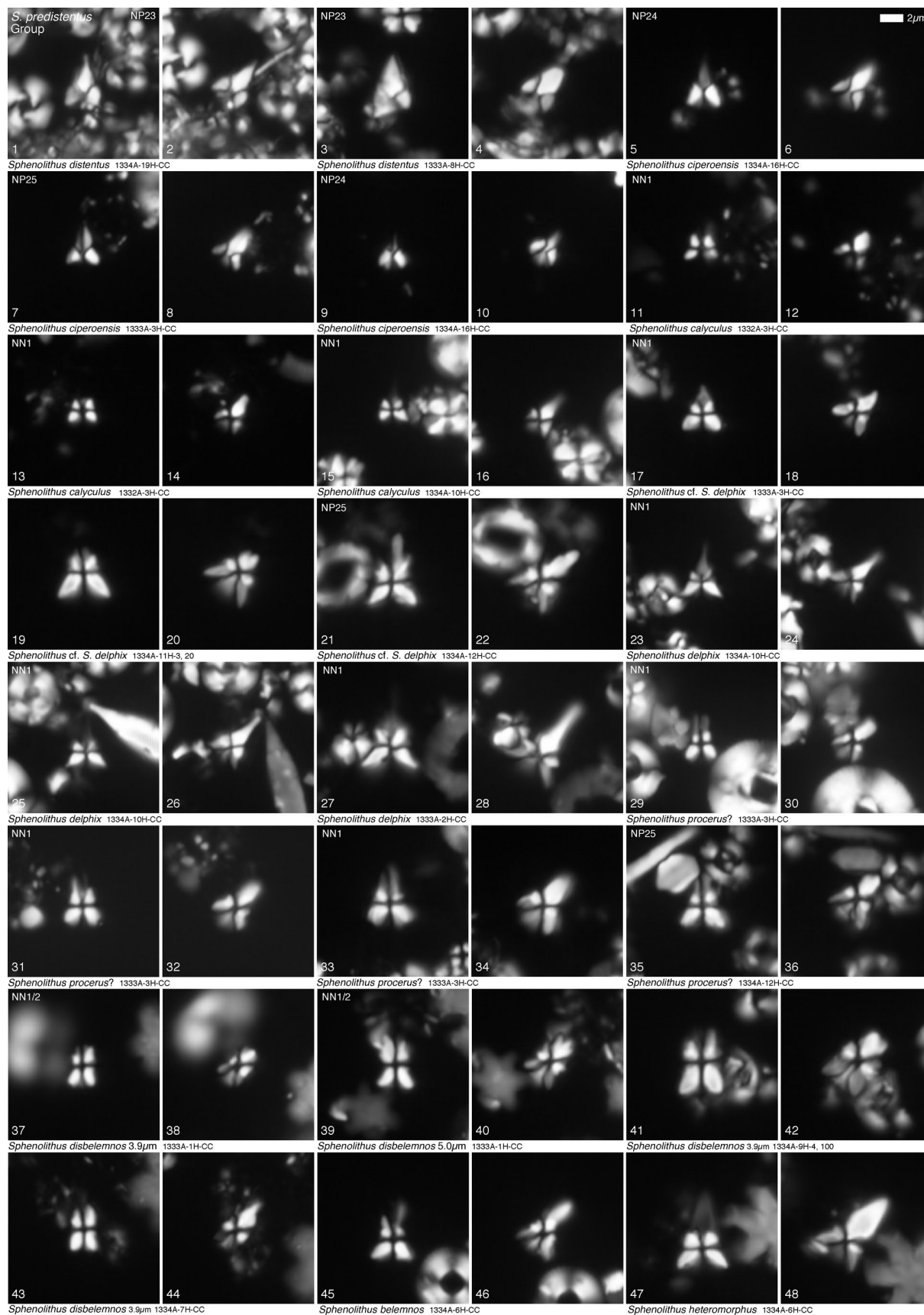


Plate 13

Sphenolithus moriformis Group, Incertae sedis nannoliths

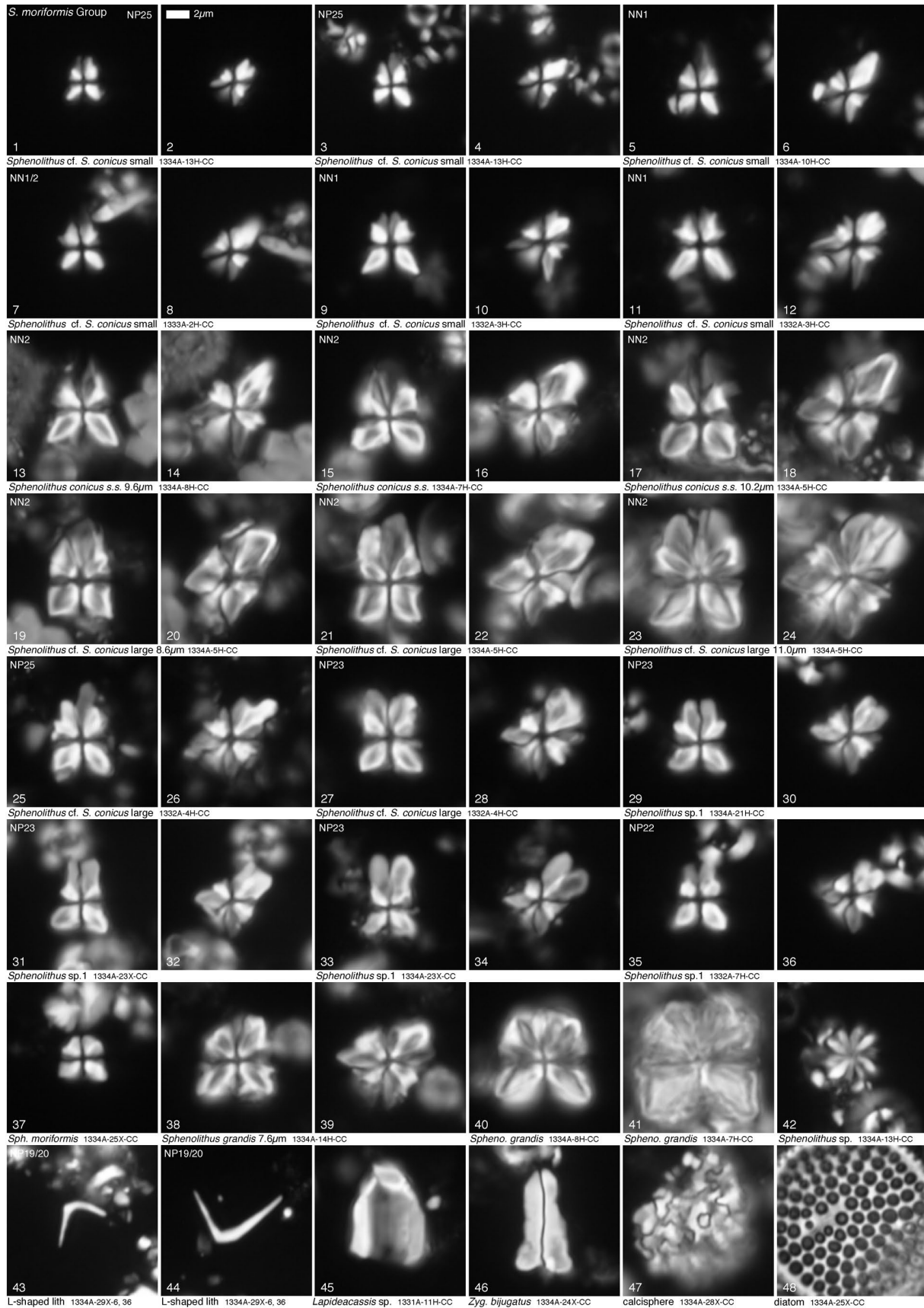


Plate 14

Incertae sedis nannoliths

